Digest

Cryo-EM as a powerful tool for drug discovery

John H Van Drie[a,*], Liang Tong[b,*]

[a] *Van Drie Research LLC, 109 Millpond, North Andover, MA 01845, USA*
[b] *Department of Biological Sciences, Columbia University, New York, NY 10027, USA*

ABSTRACT

The recent revolution in cryo-EM has produced an explosion of structures at near-atomic or better resolution. This has allowed cryo-EM structures to provide visualization of bound small-molecule ligands in the macromolecules, and these new structures have provided unprecedented insights into the molecular mechanisms of complex biochemical processes. They have also had a profound impact on drug discovery, defining the binding modes and mechanisms of action of well-known drugs as well as driving the design and development of new compounds. This review will summarize and highlight some of these structures. Most excitingly, the latest cryo-EM technology has produced structures at 1.2 Å resolution, further solidifying cryo-EM as a powerful tool for drug discovery. Therefore, cryo-EM will play an ever-increasing role in drug discovery in the coming years.

These are exciting times for our ability in drug discovery to exploit the 3D structure of the macromolecular target. Structure-based drug discovery (SBDD) began in the 1980s, when both X-ray crystallography and molecular modelling were first introduced into drug discovery; by the 1990s SBDD had matured into a routinely used approach. The first major success of SBDD was the discovery of HIV protease inhibitors against AIDS; this pandemic began in 1981 and became a huge threat by the mid-90s, when the introduction of both HIV reverse-transcriptase (RT) inhibitors and HIV protease inhibitors began to turn AIDS into a manageable disease (Fig. 1)[1]. Indeed, this is a success story for the pharmaceutical R&D enterprise as a whole, in terms of our ability to respond to a pandemic.

A revolution in structural biology has occurred in the past few years, due to dramatic advances in the technology of electron microscopy (EM) at cryogenic temperatures - cryo-EM. Not that long ago, EM was often disparaged as 'blob-ology', due to the low resolution of the structures; these were useless for drug discovery. Fig. 2 shows how structural information has improved over the years for the ribosome, in parallel with advances in X-ray crystallography and EM.

- Fig. 2A shows the first EM structure of the ribosome from 1984[2].
- Fig. 2B shows the EM structure in 1995[3,]
- Fig. 2C the X-ray density in 1998[4,]
- Fig. 2D the X-ray structure from 2000[5,]
- Fig. 2E a 2008 X-ray structure showing atomic detail how the antibiotic linezolid binds to the ribosome[6] and finally
- Fig. 2F shows a recent cryo-EM structure[7], which now displays the

various components of the complex (mRNA, tRNA, the emerging polypeptide chain).

Improvements on multiple fronts in EM have brought EM structures to the resolution where they are now useful for drug discovery. The 2017 Nobel Prize in Chemistry was awarded to Dubochet, Frank and Henderson, in recognition of their contributions to these improvements that transformed the low-resolution EM into the high-resolution cryo-EM[8]. Some of these improvements were: the ability to rapidly capture the undistorted macromolecule in vitrified ice, the ability to deconvolute the multiple conformations and orientations of the molecule in that vitrified state, and improvements in the instrumentation, especially the sensitivity of the detectors.

Cryo-EM and X-ray crystallography are complementary techniques; each facilitates the other. Compared to X-ray crystallography, cryo-EM provides a number of advantages:

(1) capturing large complexes containing multiple proteins is routine, allowing the capture of a protein in its native milieu vs. the study of a protein in isolation in crystallography,
(2) the protein is usually captured in a near-native state, something especially important in transmembrane proteins, like ion channels and G-protein-coupled receptors (GPCRs);
(3) conformational changes are routinely obtained, making clear the manner in which the target is a 'molecular machine'. This often exposes unanticipated drug binding sites, or leads to transformational insights into mechanism, or opportunities for selectivity;

* Corresponding authors.
E-mail addresses: john@vandrieresearch.com (J.H. Van Drie), ltong@columbia.edu (L. Tong).
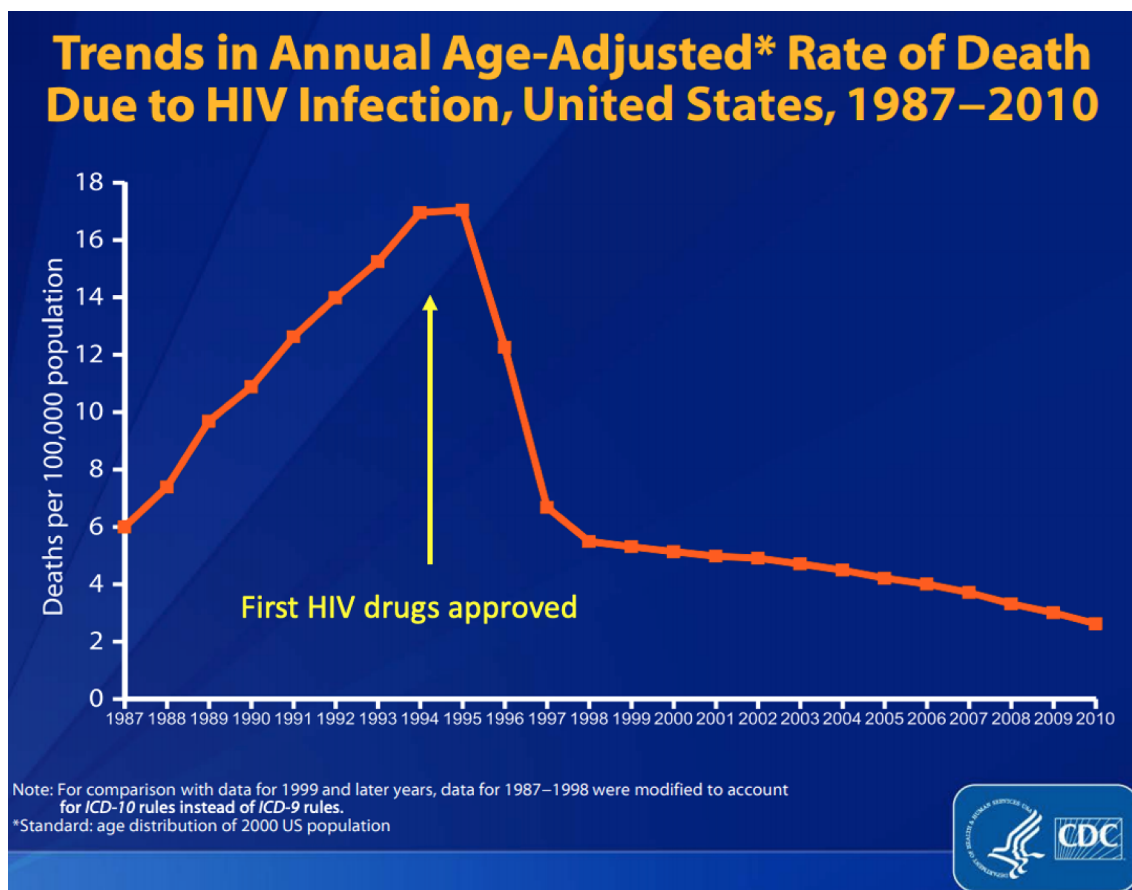
Fig. 1. Deaths due to AIDS in the US were climbing dramatically, until the introduction of drug therapies in the mid-1990s. (adapted from original graph from cdc.gov).

(4) some important off-targets of drugs can now be incorporated into the SBDD approach, e.g. ion channels and transporters; and

(5) the timeline for determining these structures can be more predictable, because crystallography requires a crystal, which is a serious bottleneck, while cryo-EM can work with the sample directly.

The primary disadvantage is that today the resolution of many cryo-EM structures is still only comparable to a low-resolution X-ray structure. However, this is changing rapidly (Fig. 3), and some recent structures have 1.2 Å resolution[9,10], comparable to the best macromolecular X-ray structures. Fig. 3 shows the growth in the number of publicly available cryo-EM structures and their improving resolution in the past decade. (We are fortunate that most funding agencies and journal policies insist that published structures are made publicly available).

There are many reviews on cryo-EM structural biology[11–19]. What differentiates this review is our focus on examples of how cryo-EM structures have impacted drug discovery, in terms of both driving the discovery of new compounds and defining the mechanism of action of known drugs. Some examples are described in detail; others are summarized briefly in a later section. There are two major challenges to compiling such a review: the literature is growing at an astonishing pace, and many examples of uses of cryo-EM for SBDD are still proprietary, but are expected soon. In each case, we will highlight many of the points made above, in terms of the special advantages of cryo-EM, and will primarily highlight examples where crystallography has fallen short of what is required.

Brief description of cryo-EM technology: Structure determination by cryo-EM typically proceeds through the following steps:

1. Isolation and purification of the sample, from natural and/or recombinant sources. This step is similar to that needed for crystallography, but the amount of sample required for EM is much smaller. Typically, several microliters at ~1 mg/ml concentration would be sufficient.

2. Screening of the quality of the sample by negative stain and/or cryo-EM. A sample displaying good conformational homogeneity can proceed to data collection, while a poor-quality sample will require optimization of the sample and/or the cryo-EM grid preparation. This is often the time-consuming part of a structure determination by cryo-EM.

3. Data collection, image analysis and reconstruction. With good quality grids, cryo-EM images (movies) can be acquired and analyzed, which ultimately could lead to a three-dimensional reconstruction revealing the structure of the sample. The image analysis and reconstruction require significant computing power, but the software is becoming more and more powerful and automated[20–23]. This step typically can be completed within a few days to a week or two.

4. Model building, refinement and analysis. The powerful tools that have been developed for model building and refinement for crystallography can be used for building and refining atomic models into cryo-EM reconstructions[24–26]. Additional tools have been developed to deal with the lower resolution cryo-EM (and crystallography) maps[27] as well as for visualization and model fitting[28].

Most importantly for drug discovery, recent improvements in both hardware and software have allowed cryo-EM structures to provide visualization of bound small-molecule ligands in the macromolecules (Fig. 4). In fact, nearly half of the ~1200 cryo-EM structures deposited
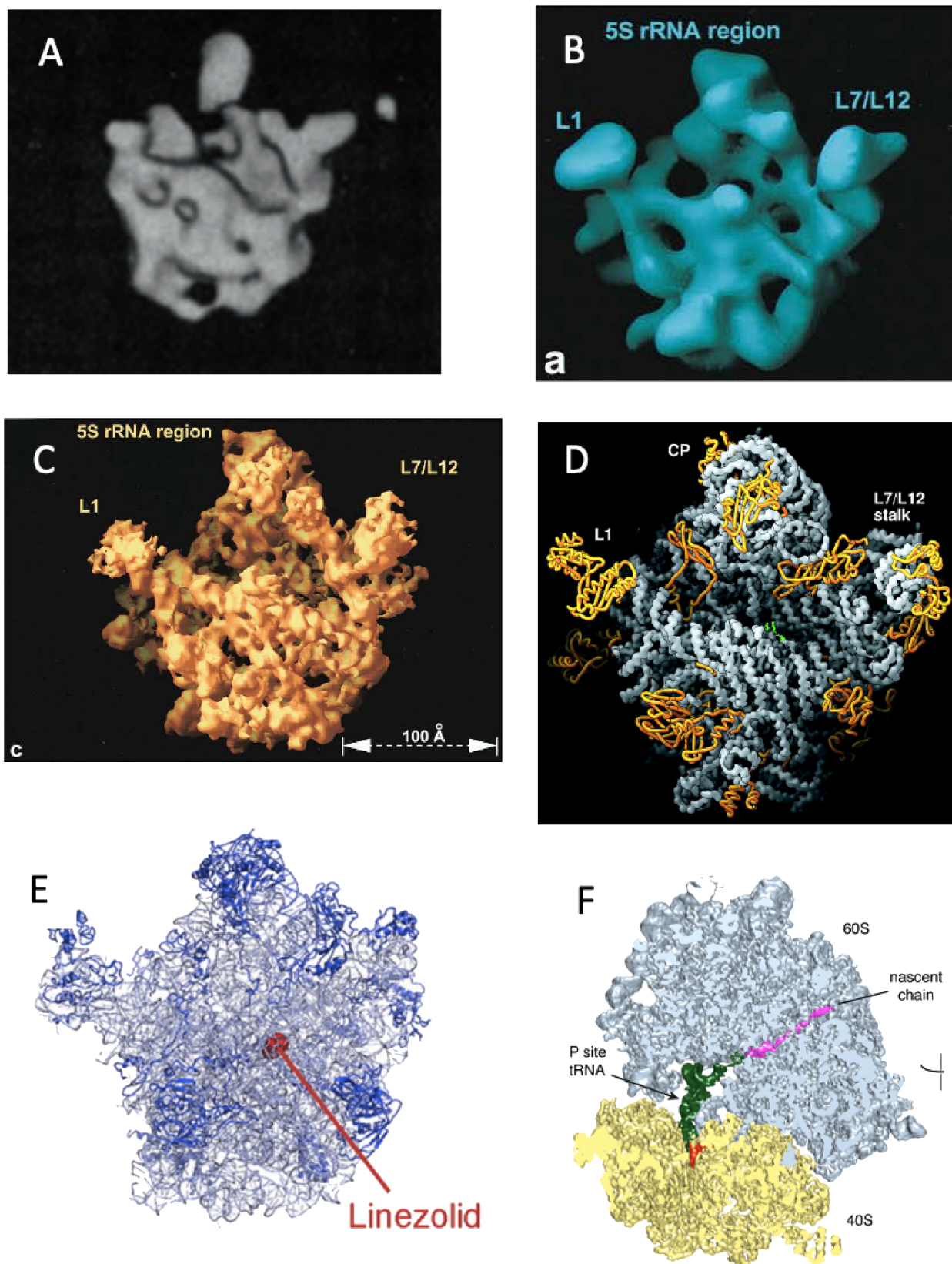
Fig. 2. Progression of resolution of ribosome structures 1984–2019. (A). the first EM structure of the large subunit of ribosome[2]; (B). 20 Å EM structure of the large subunit[3]; (C). 9 Å X-ray structure of the large subunit[4]; (D). 2.4 Å X-ray structure of the large subunit[5]; (E). a 3.5 Å X-ray structure of the antibiotic linezolid bound to the 50S subunit[6]; (F). a cryo-EM structure of the full ribosome at 2.4–3.5 Å.[7] The nascent polypeptide chain is shown in magenta, and mRNA density is shown in red (it protrudes in the direction of the viewer). The P site tRNA is green, the small subunit in yellow, and large subunit in light blue. (composite figure, from individual figures reprinted with permission).
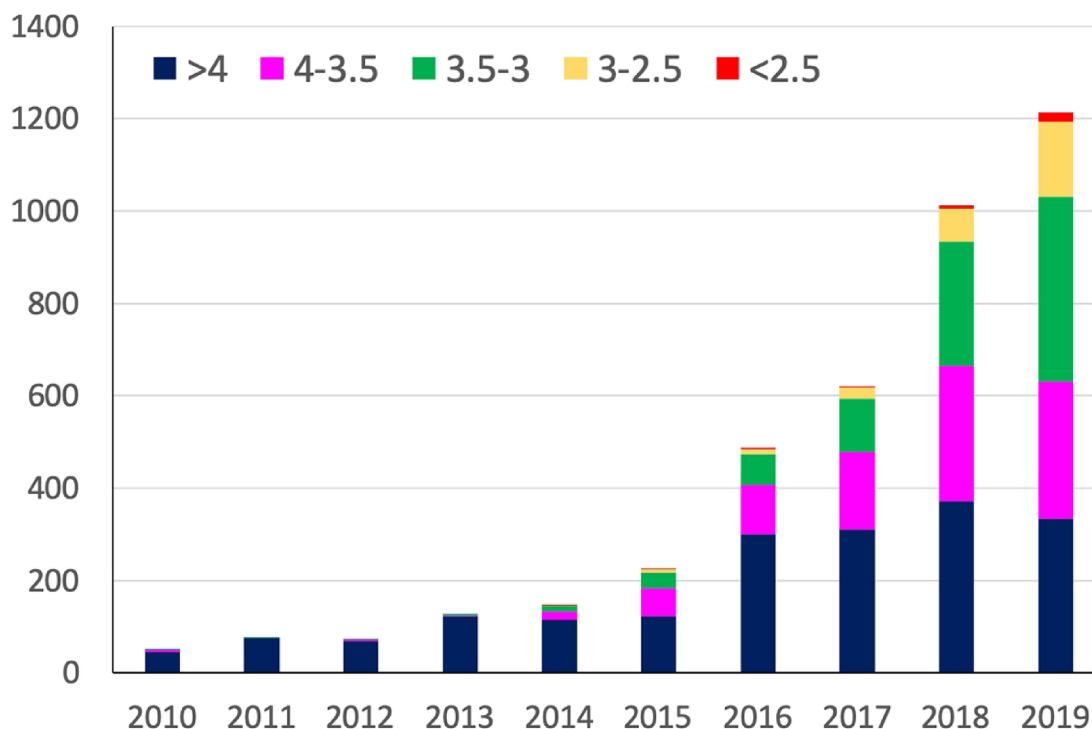
Fig. 3. Histogram of cryo-EM structures deposited in the PDB over the past 10 years (2010–2019). The bar shows the number of structures deposited in each year, divided into four categories based on the reported resolution of the structures, lower than 4 Å (dark blue), 4 to 3.5 Å (pink), 3.5 to 3 Å (green), 3 to 2.5 Å (yellow), and above 2.5 Å (red).

in the Protein Data Bank (PDB) in 2019 are at better than 3.5 Å resolution, and the number of structures at better than 2.5 Å resolution has been increasing over the years (Fig. 3). Experience has shown that EM structures between 4 and 3.5 Å resolution can already have well-defined density for the bound ligands. Most excitingly, cryo-EM reconstructions at 1.2 Å resolution have been obtained using the latest technology[9,10]. This demonstrates that there is no inherent limitation to achieving atomic resolution by cryo-EM, further solidifying cryo-EM as a powerful tool for drug discovery.

Detailed description of selected cryo-EM structures: ATP-citrate lyase (ACLY). ACLY catalyzes the conversion of citrate and CoA to oxaloacetate and acetyl-CoA, which also requires the hydrolysis of ATP. It is a major source of acetyl-CoA in the cytoplasm, and a potential target for drug discovery against dyslipidemia and cancer[29,30]. Bempedoic acid (ETC-1002) has been approved for the treatment of hypercholesterolemia[31], validating ACLY as a drug discovery target. This compound has a linear C15 di-acid backbone and needs to be converted to the CoA ester in the liver for its inhibitory activity against ACLY, which likely occurs through binding to the active site.

A series of low nanomolar ACLY inhibitors has recently been disclosed by Nimbus Therapeutics, and they are competitive against the citrate substrate of the enzyme[32]. The structure of one of these inhibitors (NDI-091143) in complex with human ACLY was determined by cryo-EM at 3.67 Å resolution in the Tong lab (Figs. 4A, 5A)[32]. Remarkably, the compound is bound in an allosteric cavity, in the hydrophobic core of the citrate binding domain of the enzyme and has no overlap with citrate (Fig. 5B). A large conformational change in the domain is required for the compound to bind, which indirectly competes against citrate. Especially, Arg379 interacts with the citrate but clashes with the inhibitor. It moves by 12 Å upon inhibitor binding (Fig. 5B). Ile344 moves by 6 Å upon inhibitor binding, and its new position clashes with citrate. The binding cavity does not exist without this conformational change. Free-energy perturbation calculations based on the binding mode of this compound can explain the binding affinities of other compounds in the series[32], supporting the structural

observations and indicating that a structure at this resolution could be useful for explaining the SAR of the compounds and drug design. In fact, extensive efforts at determining the binding mode of this compound by crystallography were not successful, and therefore cryo-EM enabled the breakthrough on this compound.

GPCRs. GPCRs (G-protein-coupled receptors) are one of the oldest targets for drug discovery. Structural data on GPCRs have exploded in the past 20 years, starting with the X-ray structures of rhodopsin[33] and the beta-2 adrenergic receptor[34]. Crystallography, cryo-EM, and NMR have all contributed to a wealth of knowledge on the details of structure and mechanism of existing drugs, which have led to the design of improved molecules[35].

There are many examples of cryo-EM structures of GPCRs that we could describe in this review. We will discuss one here in detail, GLP-1R; others will be described in brief in the following section.

GLP-1R. GLP-1R is the receptor for the gastrointestinal peptide hormone GLP-1, a key component of insulin regulation. Peptides based on GLP-1 have long been on the market for treatment of diabetes[36]. Most other drugs have been discovered via peptidomimetic approaches, targeting the orthosteric site where GLP-1 binds. Activity in the past 10 years has focused on non-peptidic molecules originating from HTS hits, functioning as positive allosteric modulators (Fig. 6), but these molecules are sub-optimal in many ways[37–39]. Upstream of GLP-1R, the "gliptin" drugs inhibit DPP-IV, the peptidase responsible for the cleavage and inactivation of GLP-1.

What makes this example of the cryo-EM structure of GLP-1R especially compelling is that it exemplifies all the advantages of cryo-EM: (1) the full structure highlights aspects that were not apparent in the X-ray structures of the individual components; (2) the key conformational change upon ligand binding and activation is now apparent; (3) this structure is significantly different than what had been anticipated via homology models, and (4) based on the state of the art, it is poised to drive the discovery of much improved drug candidates. The first cryo-EM structure of GLP-1R was published in 2017[40],Fig. 7.

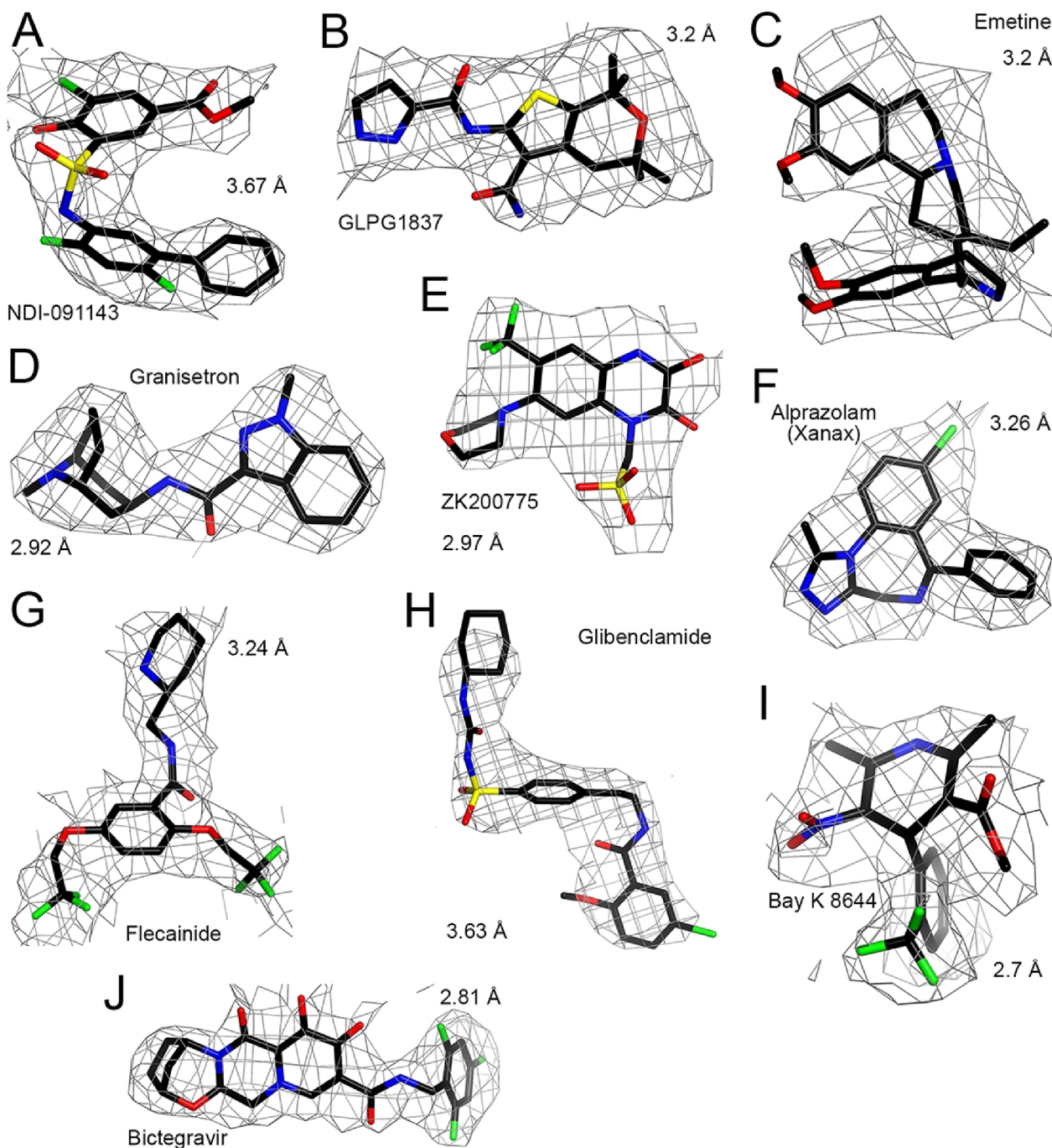In contrast to earlier work, this new cryo-EM structure shows the

Fig. 4. Observed cryo-EM density for selected drug-like ligands. (A). NDI-091143 with human ACLY. (B). GLPG1837 with human CFTR. (C). Emetine with *P. falciparum* 80S ribosome. (D). Granisetron with mouse 5-HT$_{3A}$ serotonin receptor. (E). ZK200775 with rat GluA2 AMPA receptor. (F). Alprazolam (Xanax) with human GABA$_A$ receptor. (G). Flecainide with rat Na$_v$ 1.5 voltage-gated sodium channel. (H). Glibenclamide with rat pancreatic K$_{ATP}$ potassium channel. (I). Bay K 8644 with rabbit Ca$_v$1.1 voltage-gated calcium channel. (J). Bictegravir with SIV intasome. The cryo-EM density is shown as a cage (in gray), and the compounds are shown as stick models; black (C), blue (N), red (O), yellow (P or S), green (Cl or F). The resolution of the cryo-EM reconstruction is indicated. Produced with PyMOL (www.pymol.org).

full seven transmembrane (TM) domain portion of the receptor, the *N*-terminal domain, the peptide ligand, and the G protein which transduces the signal. The structure, coupled to other biophysical and enzymatic data, clarifies how peptide binding at the extracellular surface is communicated to the intracellular receptor side: conformational changes in the transmembrane domain result in a sharp kink in the middle of TM helix 6, which pivots its intracellular half outward to accommodate the α5 helix of its G-protein. In that publication, the binding site of the known allosteric modulators could only be modelled,

by homology to other GPCRs with modulators bound. In addition, it is thought that this structure may be a paradigm for the structure of other family B GPCRs, highlighting a general mechanism whereby a flexible *N*-terminal domain outside of the membrane folds to form the binding site for the endogenous ligand. This structure also allowed them to propose a mechanism of activation. Finally, the interaction with the G-protein suggests a molecular basis for the "biased signaling" that is seen in the allosteric modulators, namely that the ratio of signaling in multiple downstream pathways differs from molecule to molecule.
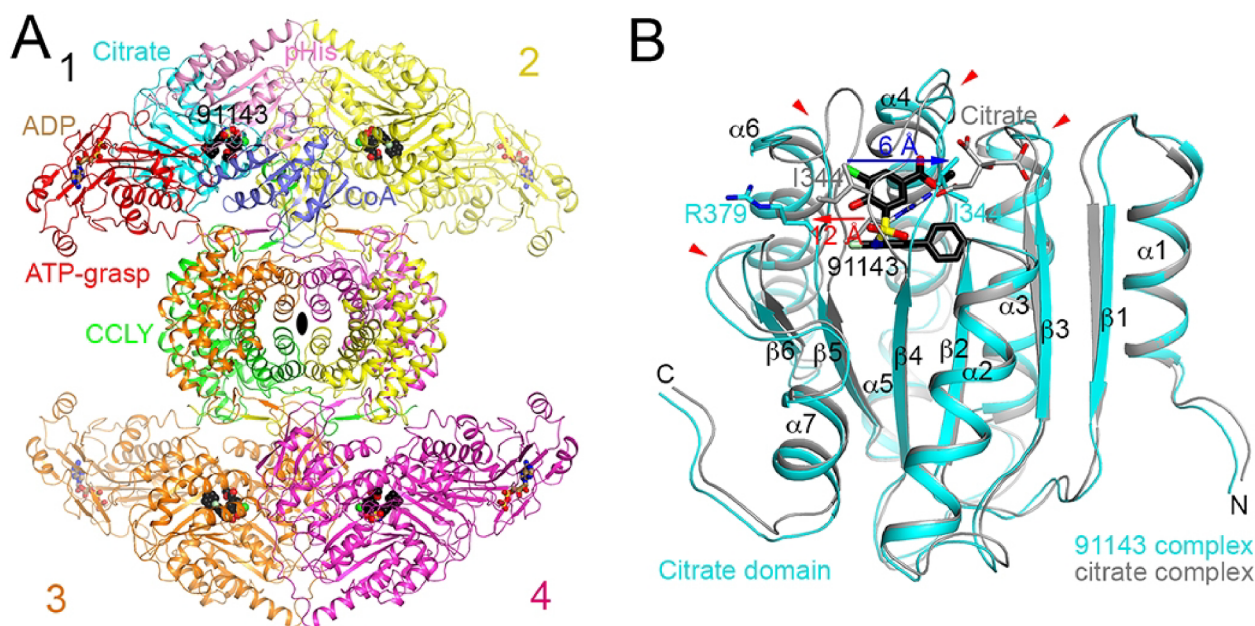
Fig. 5. Structure of human ACLY in complex with NDI-091143. (A). Schematic drawing of the structure of human ACLY tetramer in complex with NDI-091143. Monomer 1 is colored by its domains and labeled, monomer 2 in yellow, monomer 3 in orange and monomer 4 in magenta. NDI-091143 is shown as a sphere model (carbon atoms in black). (B). Extensive conformational changes in the citrate domain of ACLY is required for inhibitor binding. Regions of large conformational changes are indicated with the red arrow heads, and those for Arg379 and Ile344 are indicated with the red and blue arrows, respectively.

A series of new GLP-1R allosteric modulators has appeared from vtv Therapeutics (the company formerly known as Trans Tech Pharma). The first of these compounds TTP054 was tested in Phase 2 clinical trials, but there is no evidence that it continued on phase 3[38,41]. However, newer analogs of these molecules are now in Phase 2, e.g. TTP054-201, and the cryo-EM structure of an analog has been published this year[42],Fig. 8, This structure shows the same overall conformation as the earlier cryo-EM structure, but now shows the location of the ligand. Of course, others are in this race as well, e.g. Pfizer's PF-06882961, which has been disclosed briefly, but apparently not in conventional scientific literature.

In addition, GLP-1R has been implicated in some CNS disorders, like AD and PD[36]. Additional work on GPL-1R allosteric modulators driven by this cryo-EM structure may allow further optimization for these indications.

Ion channels. Ion channels control the conduction of signals in nerves and are one of the oldest drug targets. They have been a rich source for structural biologists as well, starting with the first major breakthrough in 1998 with the publication of the X-ray structure of the potassium channel by Rod MacKinnon and colleagues[43]. Three examples which most strongly exemplify the strengths of cryo-EM will be discussed in detail here: TRP channels, CFTR, and hERG. In each case, novel insights into mechanism have arisen by understanding the conformational changes in these molecular machines. In addition, they are the targets of important new drugs, and are being actively pursued by many drug discovery groups. Unfortunately, in each case there is little in the public literature that describes how these structures are being exploited in drug design.

TRP channels. The TRP channels (Transient Receptor Potential channels) mediate pain and temperature signals, and have been pursued recently as a target for neuropathic pain, migraine, and inflammatory pain; multiple drug candidates are being evaluated in clinical studies[44] TRPV1 is the receptor to which capsaicin binds (the active substance in hot chili peppers), and has been described as the "'poster child' for elucidating basic principles underlying TRP channel function and structure". Its structure was first determined via cryo-EM by the Julius lab at UCSF (Fig. 9)[45,46]. Cryo-EM is spurring an on-going revolution in this area[47]. It has enabled the determination of a large number of TRP channel structures (Table S1).

This initial cryo-EM structure was noteworthy for multiple reasons. It gave the first, approximate picture how capsaicin and related molecules bind; the second publication gave the atomic-level detail of the ligand-protein complex. These publications also showed multiple functional states, allowing hypotheses to be formed on the mechanism of activation (Fig. 10A). While the overall architecture resembled other channels like the potassium channel, the mechanism of activation was startlingly different from what was known from other channels, pointing to an unusual allosteric coupling from the ligand-binding S1-S4 helices (homologous to the voltage-sensing domain in voltage-gated ion channels) to the pore-forming domains. These differences are critical to achieving selectivity between and among these families of channels and contributed to the ability to design out the side effects of the first TRPV1 antagonists discovered[48]. These experiences exemplify the power of cryo-EM in drug discovery: (1) multiple conformational states can readily be determined, often in one experiment, (2) these states lead to mechanistic hypotheses, which in turn lead to (3) insights into how to achieve selectivity for the channel of interest.

One example of a medicinal chemistry effort exploiting this structure is from a group in Seoul, S Korea, who have published extensively on a series of analogs designed using this cryo-EM structure (Fig. 10B)[49,50] They achieved sub-nM activity and excellent activity in a neuropathic pain model at 10 mg/kg.

The Cystic Fibrosis Transmembrane Conductance Regulator (CFTR). Cystic Fibrosis is a fatal lung disease, which was found in 1989 to originate from a single mutation in one gene, expressing a protein which was later found to regulate chloride levels, given the name CFTR[51–53]. One mutation, F508del, accounts for the majority of patients, though disease mutations occur in many positions in CFTR. The first CF drugs directly targeting CFTR were discovered by Vertex Pharmaceuticals[54–55]: ivacaftor, approved in 2012, followed by lumacaftor, and tezacaftor, which now form the standard-of-care as a triple combo, Trikafta, approved in 2019. The Vertex drugs were all discovered empirically, in heroic medicinal chemistry efforts[56], exploiting a high-throughput cell-based assay. No knowledge of the receptor structure was exploited, except to select specific cell lines with certain mutations. Despite their great commercial success, Vertex has thus far
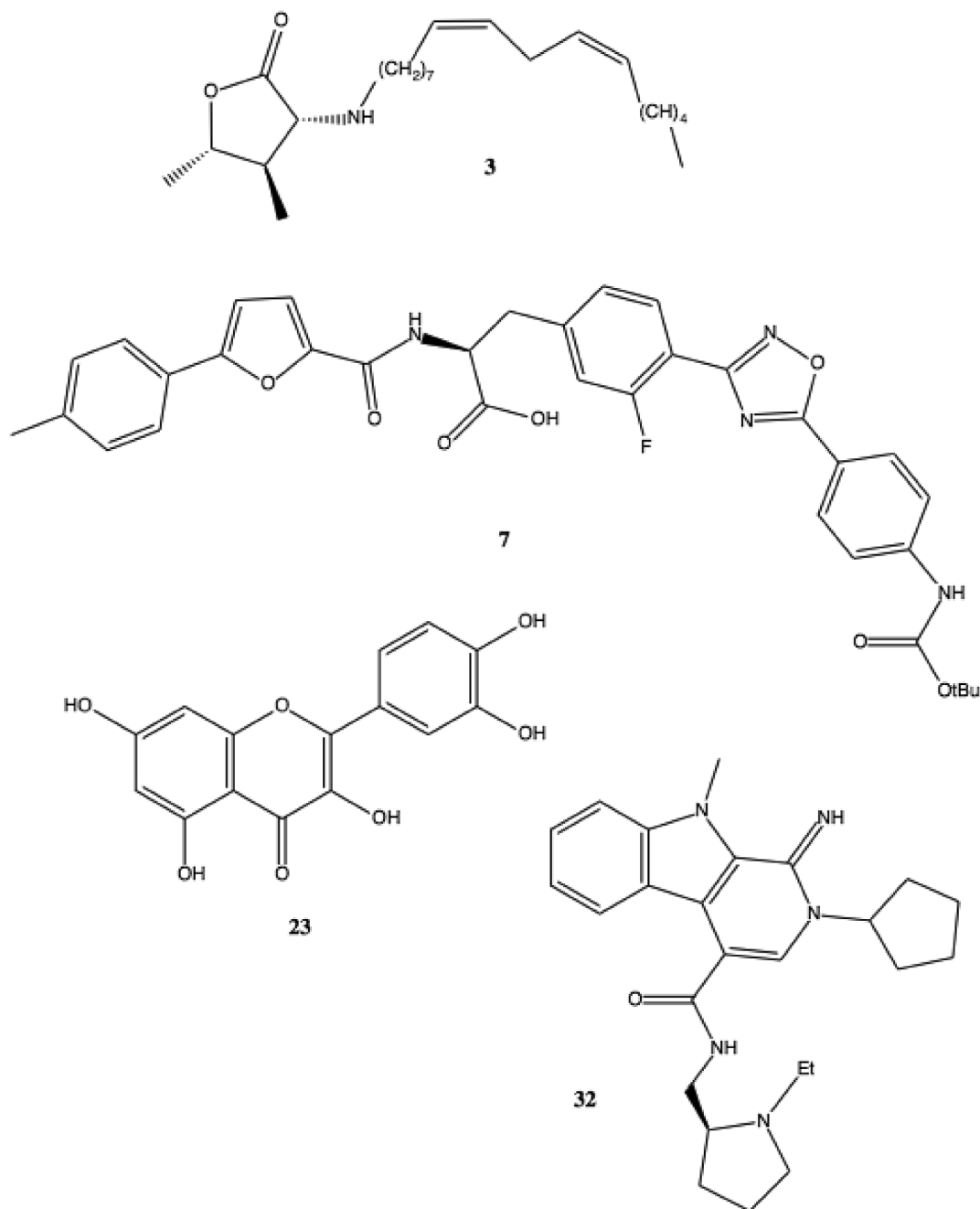
Fig. 6. Some GLP-1R allosteric modulators (numbering as in[37].

attracted little competition, suggesting that this is a challenging area for drug discovery.

All efforts to crystallize CFTR, the first step to determining an X-ray structure, have failed. However, the lab of J. Chen at Rockefeller has used cryo-EM to determine increasingly useful structures of CFTR: first from zebrafish[57]; then human[58] with some domains unresolved; then human, better-resolved with indications of the conformational changes upon channel activation[59]; and, finally, in 2019, CFTR in complex with ivacaftor, and a drug candidate discovered by Galapagos (Fig. 11)[60]. These two structurally distinct compounds bind in the same pocket, at the interface between the CFTR and the lipid membrane. The binding pocket is part of the hinge for channel gating, and the presence of the compound may stabilize the channel pore in an open configuration, explaining its potentiating effect.

Persuasive homology models of human CFTR had been built [e.g.[61] but these did not prove useful. It is difficult to convey how

astonishing this final structure of ligand-bound CFTR was to those active in CF, as all prior hints about possible ligand-binding sites pointed to regions in the nucleotide-binding domains near F508. Instead, both ivacaftor and GLPG-1837 bind to a kink in a transmembrane helix embedded in the membrane. None of the earlier structures showed either a clear kink in that helix, or a binding pocket there, and generally the notion of a binding pocket contacting the lipid bilayer is exceptional and poses special challenges to compound design.

It is in the early days, but it is reasonable to expect that this new structure will now permit structure-based optimization of such molecules. Further structures clarifying conformational changes, mechanism, etc. will undoubtedly be helpful.

As an aside, from the perspective of genomics-based small-molecule drug discovery, it is worth noting the length of time required: the mutation was identified in 1989, and not until 2012 was the first drug approved to treat the disease. And, of course, there are many other
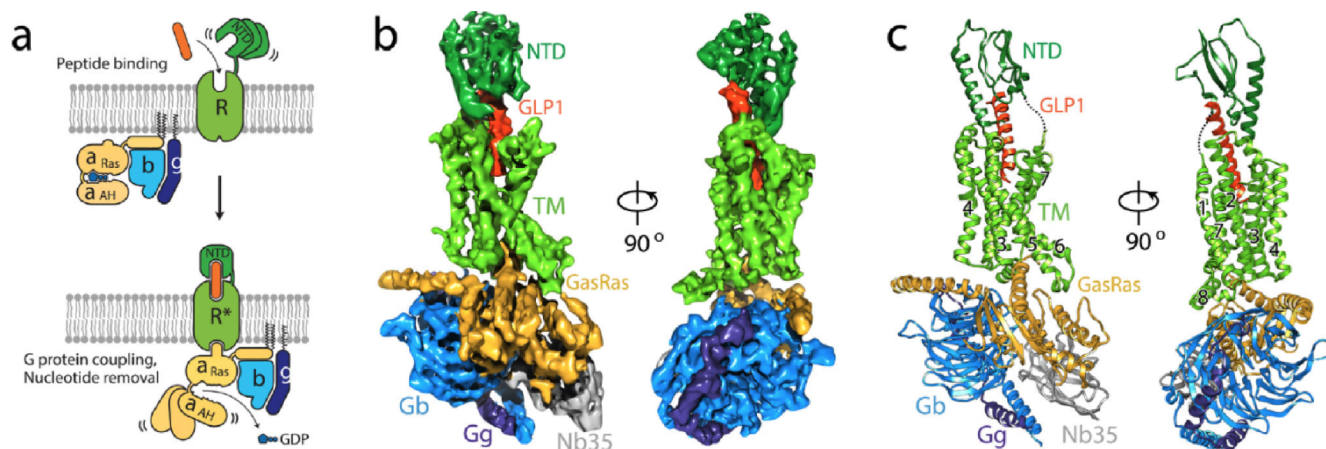
Fig. 7. Cryo-EM structure of the hGLP-1:rGLP-1R:Gs complex. a, Schematic of the activation of a family B GPCR by extracellular peptide agonist via a 'two–domain' binding mechanism. b, Views of the GLP-1R:Gs complex cryo-EM density map, colored by subunit (TM in light green, NTD in dark green, GLP-1 peptide in orange, GαsRas in gold, Gβ in light blue, Gγ in dark blue and Nb35 in grey). c, Structure of the activated GLP-1R-Gs complex in the same view and color scheme as shown in b. (from[40], reprinted with permission).
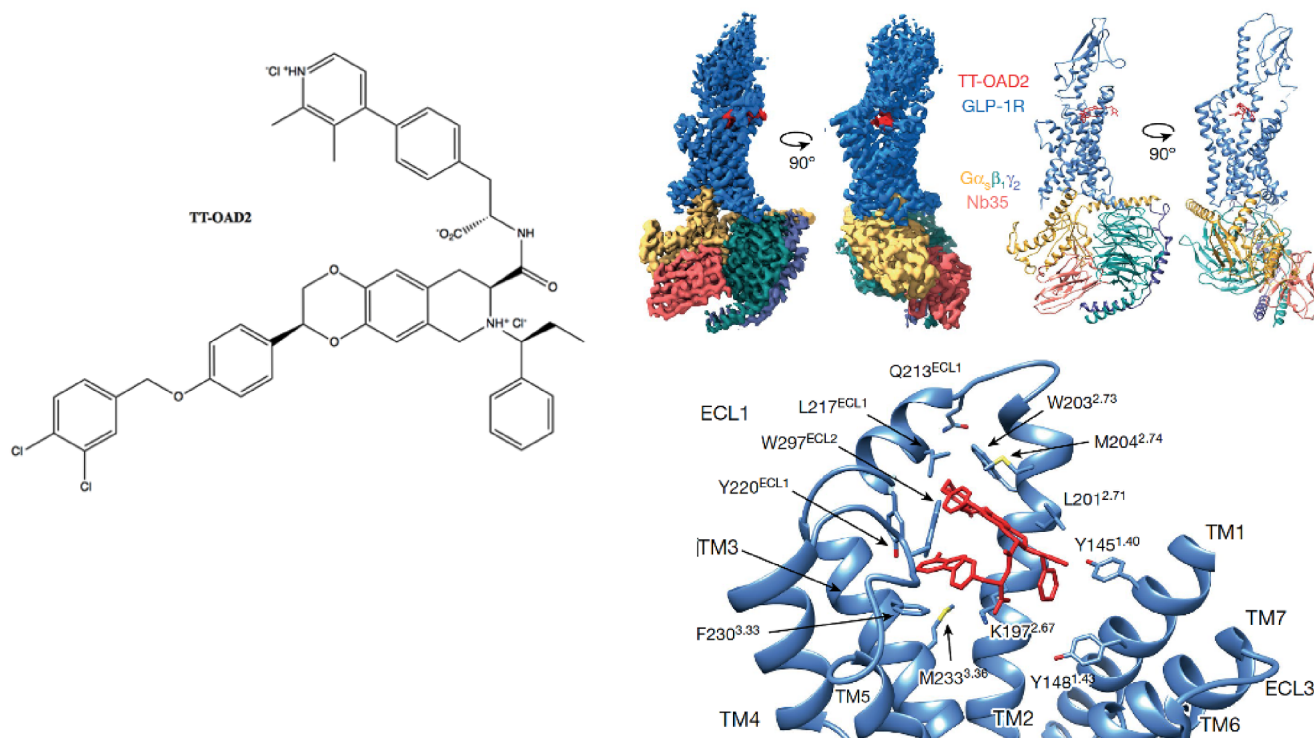

Fig. 8. The TT-OAD2–GLP-1R–Gs cryo-EM structure reveals non-peptide binding site. a. TT-OAD2. b. orthogonal views of the TT-OAD2–GLP-1R–Gs complex cryo-EM map (left) and the structure after refinement in the cryo-EM map (right), color-coded to protein chains; GLP-1R (blue), TT-OAD2 (red), heterotrimeric Gs (α: gold, β: dark cyan, γ: purple, Nb35: salmon). c. Detail of TT-OAD2 in the binding site. Interacting residues of GLP-1R (blue) with TT-OAD2 (red). (from[42] reprinted with permission).

targets where disease-causing mutations have been known for a long time but thus far no treatment is available.

hERG channel. Unwanted inhibition of the hERG channel has been a *bête noire* of drug hunters since the discovery in the mid-1990s that this channel mediates the long-QT syndrome which often leads to fatal arrhythmias[62–63] Homology modelling[64] has not shown to be especially useful in designing out the hERG liability. In 2017, a cryo-EM structure was published from the MacKinnon lab (Fig. 12)[65], which broadly showed the same architecture as that homology model - a central volume surrounded by four hydrophobic pockets - but this new detail made it clear why this channel should be so promiscuous, why a basic amine is essential, and highlights how this channel's selectivity filter is

subtly different from other known K channel structures. It is not yet evident in the medicinal chemistry literature that this structure has permitted structure-based optimization away from hERG affinity, or whether a structure with a ligand bound will be needed. It has, however, played a role in the steadily increasing ability of various software tools to estimate the long QT liability[66,67].

Viruses. Here, we will focus on one single virus, SARS-CoV-2, the cause of COVID-19, the scourge of this *annus horribilis*. The SARS-CoV-2 genome sequence was first published in January 2020[68]. Since that time, over 200 X-ray structures and 20 cryo-EM structures have been published. From the simplest perspective, the key viral proteins are
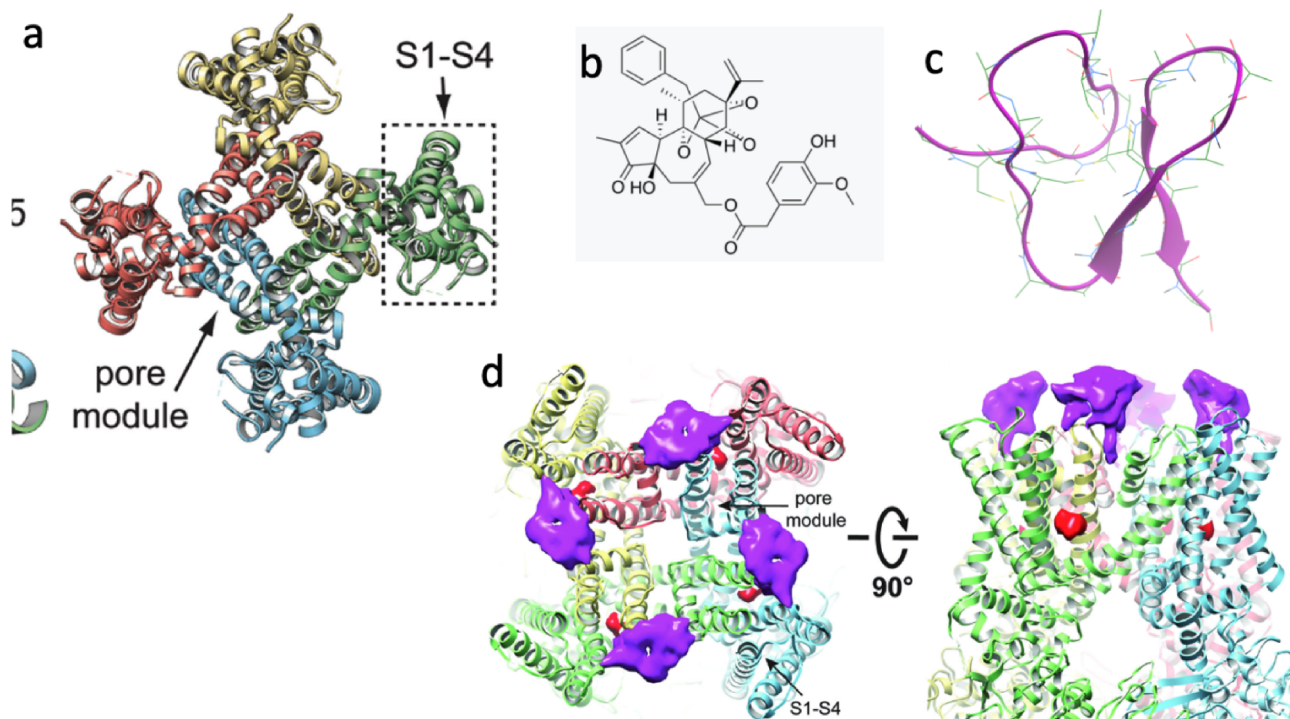
Fig. 9. Structure of TRPV1 in complex with vanilloid ligand and spider toxin. a. TRPV1 channel, bottom view. Note that S1–S4 domains flank and interact with S5-P-S6 pore modules from adjacent subunit, reminiscent of voltage-gated ion channels. b. Resiniferatoxin (RTX). c. Vanillotixin (DkTx, spider toxin). d. TRPV1 channel, bound to RTX (red sphere) and vanillotoxin (magenta). (from[46], reprinted with permission).

- the spike protein, which resides on the exterior of the virus;
- the RNA-dependent RNA polymerase (RdRp);
- the protease, which cleaves the polypeptide chain translated from the viral genome, as in HIV protease and HCV protease, which has primarily been the domain of crystallography

Drug discovery driven by these structures is still in its infancy, but the structures do highlight multiple opportunities to design inhibitors of the key steps of viral infection and propagation. Furthermore, one structure suggests the binding conformation of remdesivir, the only drug which has been authorized by the FDA for emergency use against the virus.

The spike protein. The virus gains entry into the cell via interactions between the spike proteins on the virus surface and a transmembrane protein which sits on the surface of the host cell, ACE2. The spike protein functions as a trimer and undergoes a conformational change and a series of steps to infiltrate into the cell. Many X-ray structures have appeared of the isolated spike protein, but especially compelling are the larger complexes which have been determined via cryo-EM, and ones which demonstrate the large conformational changes that occur upon activation (Fig. 13A, B)[69]

The RNA-dependent RNA polymerase (RdRp). SARS-CoV-2 is an RNA virus, encoding its genome in strands of RNA, unlike humans whose genome is encoded in DNA. Hence to replicate its genome, it requires an enzyme that is not present in the host cell, an RNA-dependent RNA polymerase (RdRp). Some known antivirals are weak RdRp inhibitors, such as the nucleoside mimics remdesivir and sofusbuvir. A cryo-EM structure has been published which allows one to form reasonable hypotheses how these molecules may bind to RdRp (Fig. 13C, D)[70]. This structure probably provides the greatest opportunity for structure-based design of COVID-19 antivirals.

The RdRp is only one component of a much larger complex, the replicase complex. A recent preprint describes a cryo-EM structure of a large section of that replicase complex[71] (Fig. 13E). Understanding the motions of this molecular machine, as RdRp 'walks' along the template RNA, may give insights into alternative ways of inhibiting the polymerase action. One new revelation from the structure is that there are extensions of the viral protein NSP-8 which interact with the paired
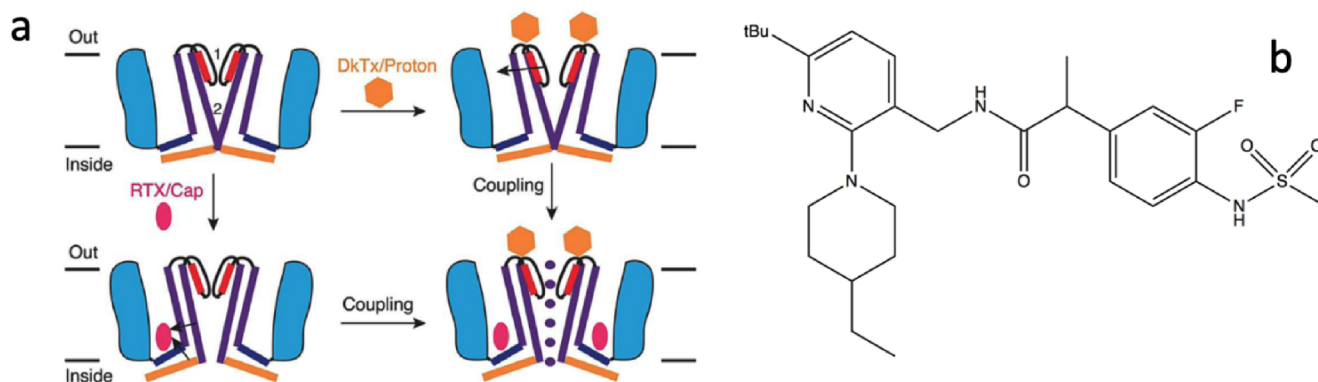

Fig. 10. a. Model for TRPV1 activation (from[46] reprinted with permission)). b. TRPV1 antagonist designed from this structure (from[49].
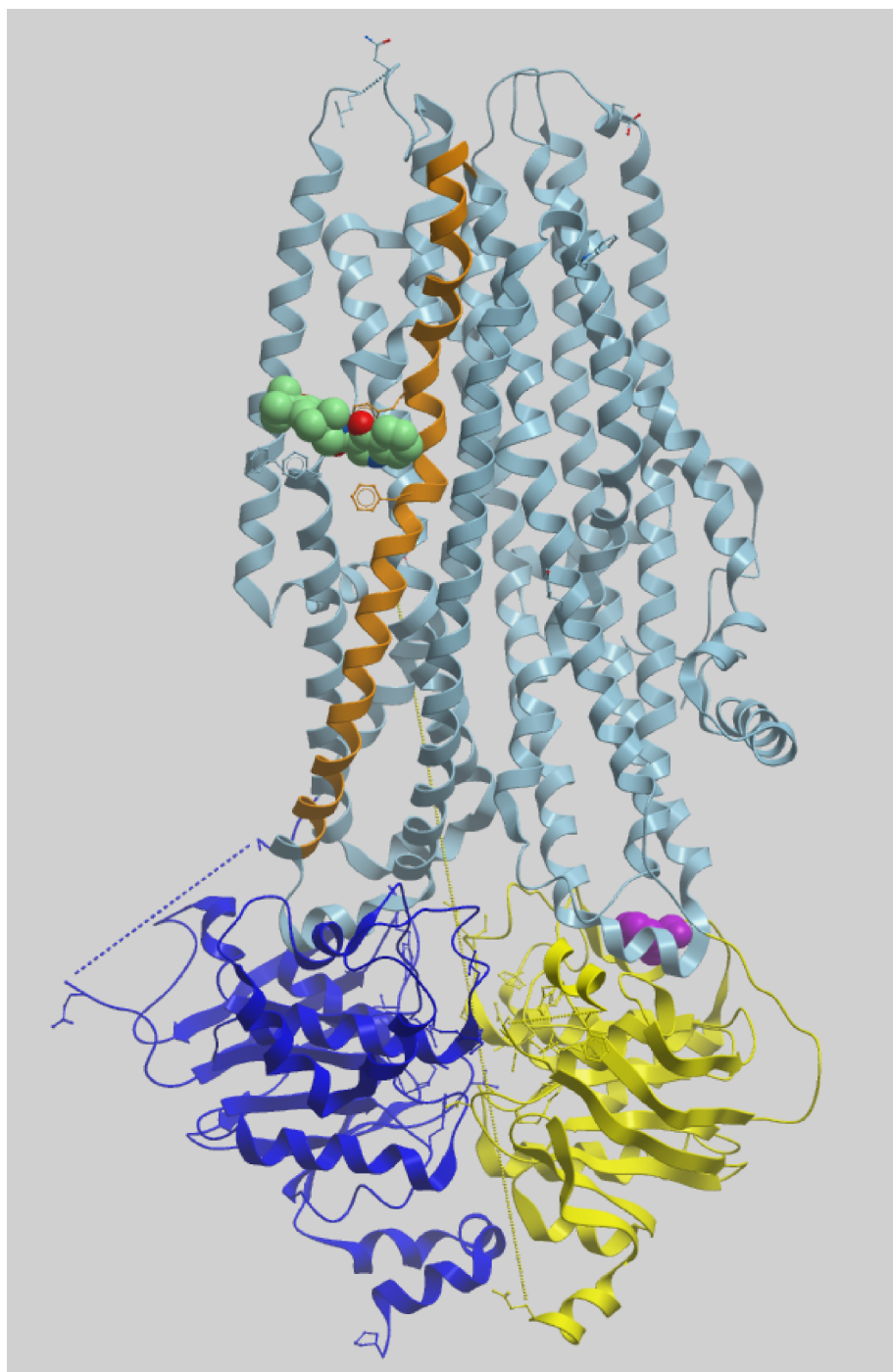
9

Fig. 11. Structure of CFTR. Ivacaftor (green) bound to CFTR, viewed from the membrane. The first nucleotide binding domain (NBD1) is in yellow. NBD2 in dark blue. The transmembrane helices are light blue, except for the kinked helix TM8 to which ivacaftor binds is shown in orange. F508 is shown in purple. The two ATP molecules, not shown, would be sandwiched in between the NBD's. (from[60], PDB code 6O2P).

RNA.

Another great opportunity lies ahead for cryo-EM in SARS-CoV-2 antivirals by looking at other mega-complexes involving host proteins, for example the enhanceosome, the target of interferon, a protein which is well-known for its antiviral activity against other viruses, and has even been demonstrated to show clinical efficacy against COVID-19[72].

Brief descriptions of additional cryo-EM structures with drug-like ligands: Overview.

Here, we describe several additional structures with drug-like small molecules bound (Table P-1). Unlike the previous section, only brief descriptions will be given due to space considerations; the readers are

referred to the original publications for detail. The cryo-EM density for some of the small molecules are also shown (Fig. 4), as an illustration of the quality of the cryo-EM reconstructions. A more complete listing of the published structures with bound drug-like small molecules is given in Table S1. Only those structures with explicitly modeled small molecules are considered here. Structures with bound biochemical ligands (substrates, substrate analogs, cofactors, prosthetic groups) are generally not included in the consideration here, although good-quality EM density can be observed for them as well. In addition, cryo-EM structures have been obtained for other drug discovery targets, such as inflammasome, but no structures of complex with drug-like molecules are
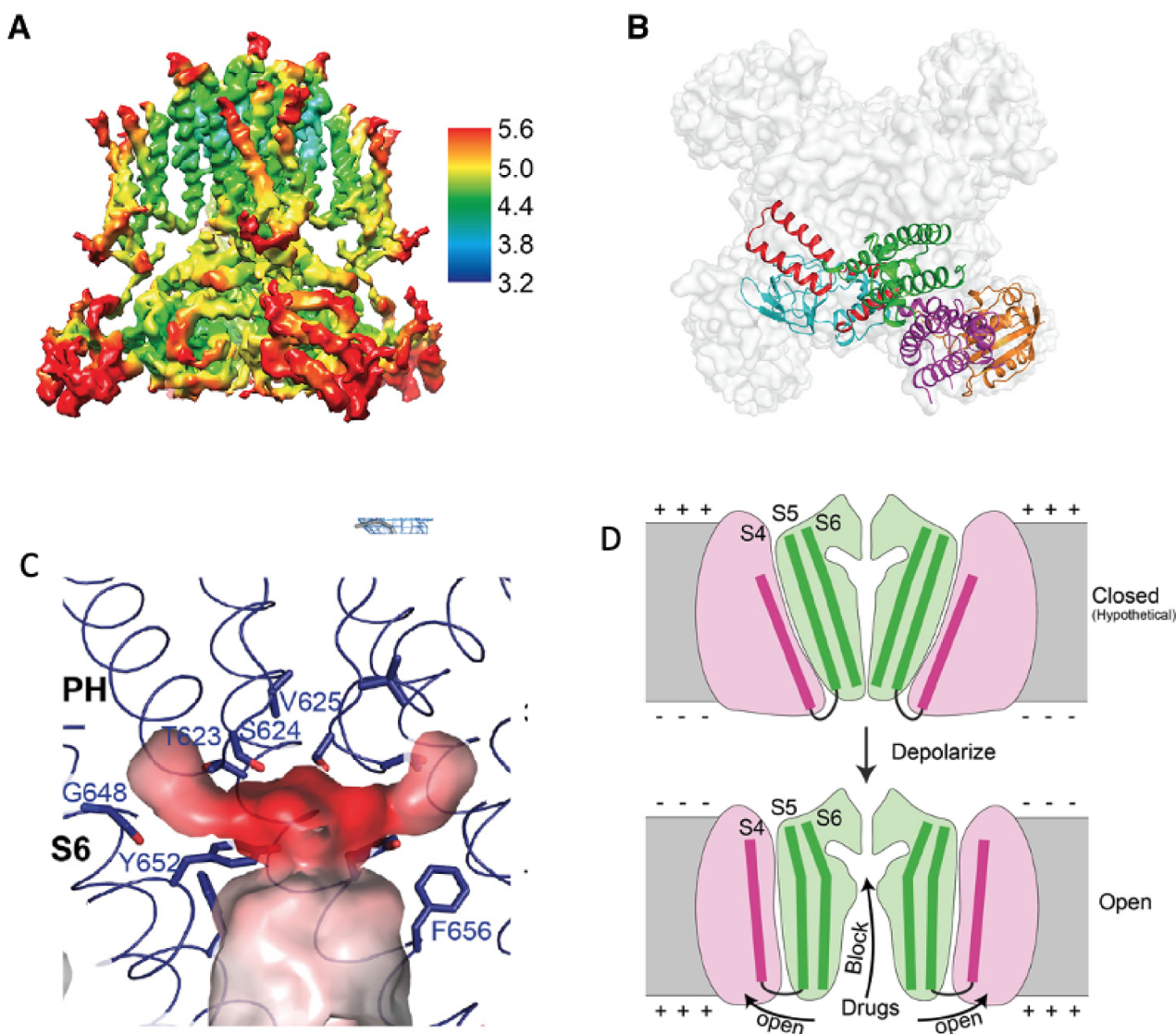
Fig. 12. Model of hERG activation and hERG blockade. (A) hERG channel, overall density, color-coded by resolution. (B) hERG overall architecture viewed down the 4-fold axis from the extracellular side. The hERG channel is represented as semi-transparent molecular surface with ribbon representation for one subunit. (D) The central cavity of hERG, shown as a translucent surface colored by eletrostatic potential. Residues related to drug binding are shown as sticks. (E) Model of hERG activation. (Figures from[65], reprinted with permission).

currently reported for them. Of course, there are likely a substantial number of structures of ligand complexes determined at pharmaceutical and biotech companies that have not yet been published or deposited in the PDB.

The analysis of deposited cryo-EM structures with bound drug-like ligands also indicates that the majority of them are for large complexes (ribosome, proteasome, spliceosome, microtubule, actin, virus, and others) and membrane proteins (receptor, channel, transporter, and others). This is a reflection of the fact that cryo-EM has made it possible (and/or more readily) to determine such structures, and the drug-like ligands probably also helped to stabilize some of the complexes for structural studies. In comparison, the number of structures of soluble enzymes is smaller, although several of them have been used to demonstrate the possibility of pushing cryo-EM to high resolution[73–75]. Nonetheless, small-molecule ligands can be observed for these targets[76], and fragment-based drug discovery by cryo-EM has recently been reported[77]. Some of these proteins are too small for the current EM technology, which favors larger molecules and complexes. Structures of smaller proteins can be determined by EM for example by complexing it with an antibody. At the same time, constant improvement in EM

technology has made it possible to determine the structures of ever smaller proteins. It is also likely that many of these structures are still being determined by X-ray crystallography, which is faster and easier if good quality crystals and compound soaking protocols are available. Routine use of high-throughput structure determination by cryo-EM, for example for lead optimization, will benefit from additional hardware and software improvement. However, if good conditions for preparing frozen grids of the sample are known, it may be envisioned that faster data collection and processing can be achieved to substantially increase the throughput of cryo-EM.

Ribosome. A large number of cryo-EM structures have been reported of ribosomes from various organisms bound to antibiotics, anti-protozoals, and other compounds (Table S1). These compounds include natural products (such as erythromycin, avilamycin, paromomycin, emetine, mefloquine) as well as synthetic molecules (such as linezolid and cadazolid). The binding modes of some of these compounds were originally determined by X-ray crystallography, but cryo-EM is now the dominant method for determining ribosome structures. For example, the binding mode of emetine is clearly defined by the cryo-EM map at 3.2 Å resolution (Fig. 4C)[78].
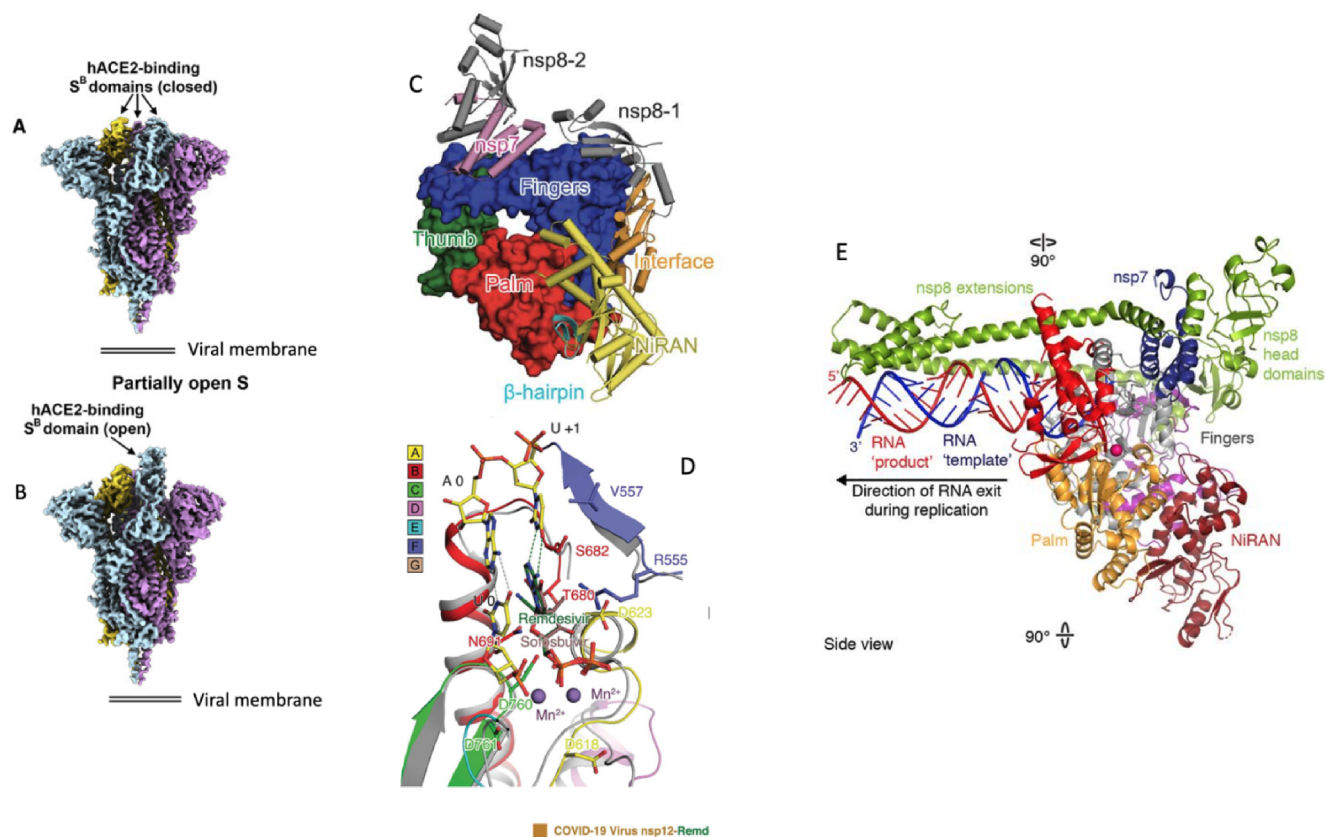
Fig. 13. (A) and (B) show the conformational changes of the spike protein trimer that occur to expose the binding domain for ACE2, as the virus encounters the host cell (from Fig. 3,[69] reprinted with permission) (C) A high-level view of the RNA-dependent RNA polymerase (RdRp), highlighting the thumb/palm/fingers domain, surrounded by accessory proteins (from Fig1B,[70]), reprinted with permission (D) A detailed view of RdRp, with a model of how the bioactive forms of remdesivir and sofosbuvir may bind. (from Fig 4[70], reprinted with permission (E) A structure of the replicase complex, of which RdRp is one part. The template RNA is shown as a blue helix; the newly synthesized strand in red. Note: the color-coding of thumb/palm/finger is different from (C). from Fig 2,[71]

Serotonin receptor. The 5-HT3 serotonin receptors are pentameric ligand-gated ion channels (pLGIC) and they are targets for therapeutic agents against nausea, vomiting, and depression[79]. The cryo-EM structures of these receptors in complex with serotonin (5-hydroxytryptamine, 5-HT) were reported recently[80–81]. Serotonin binding causes extensive conformational changes, promoting a conductive, open state. The anti-emetic drug granisetron is bound in the same site as serotonin (Figs. 4D, 14A, B)[82], but it stabilizes a closed state of the channel, distinct from the apo, resting state.

AMPA receptor. The ligand-gated ion channels AMPA-type ionotropic glutamate receptors (AMPARs) are associated with serious neurological diseases such as depression and Alzheimer's. A cryo-EM structure of the GluA2 receptor bound to the competitive antagonist ZK200775 (also known as fanapanel) was reported recently (Fig 4E)[83].

A crystal structure of this compound bound to the ligand binding domain (LBD) of the receptor is also available, at 1.25 Å resolution[84].

GABA receptor. Type A GABA (γ-aminobutyric acid) receptors (GABA$_A$ receptors) are ligand-gated chloride channels in the central nervous system and are associated with mental illnesses such as epilepsy, chronic pain, anxiety and insomnia[85]. These receptors contain many allosteric sites, and they are targets for benzodiazepines (such as diazepam/Valium and alprazolam/Xanax) and other therapeutic agents as well as for drug abuse. Competitive antagonists (such as flumazenil) are used clinically to reverse the effects of benzodiazepines, especially their overdose.

The binding modes of flumazenil[86], Valium and Xanax (Figs. 4F,15)[87] have been revealed by recent cryo-EM studies. Xanax and Valium share essentially the same binding modes, at the interface

Table P-1

Cryo-EM structures with drug-like small-molecule ligands discussed in this review.

| Drug-like ligand	Target	Resolution (Å)	PDB IDs and references
Emetine	Ribosome	3.2	3J7A[78]
Granisetron	Serotonin receptor	2.92	6NP0[82]
ZK200775 (Fanapanel)	AMPA receptor	2.97	6PEQ[83]
Alprazolam (Xanax), diazepam (Valium)	GABA receptor	3.26, 3.58	6HUO, 6HUP[87]
Resiniferatoxin	TRP channel	2.95	3J5Q, 3J5R[46]
Flecainide	Sodium channel	3.24	6UZ0[88]
Glibenclamide	Potassium channel	3.63	6BAA[90]
Bay K 8644, verapamil, nifedipine, diltiazem,	Calcium channel	2.7, 2.9, 2.9, 2.6	6JP8, 6JP5, 6JPB 6JPA[92]
Ivacaftor, GLPG1837	CFTR	3.3, 3.2	6O2P, 6O1V[60]
Bictegravir	Intasome	2.81, 2.9	6RWM[98], 6PUW[99]
NDI-091143	ACLY	3.67	6O0H[32]
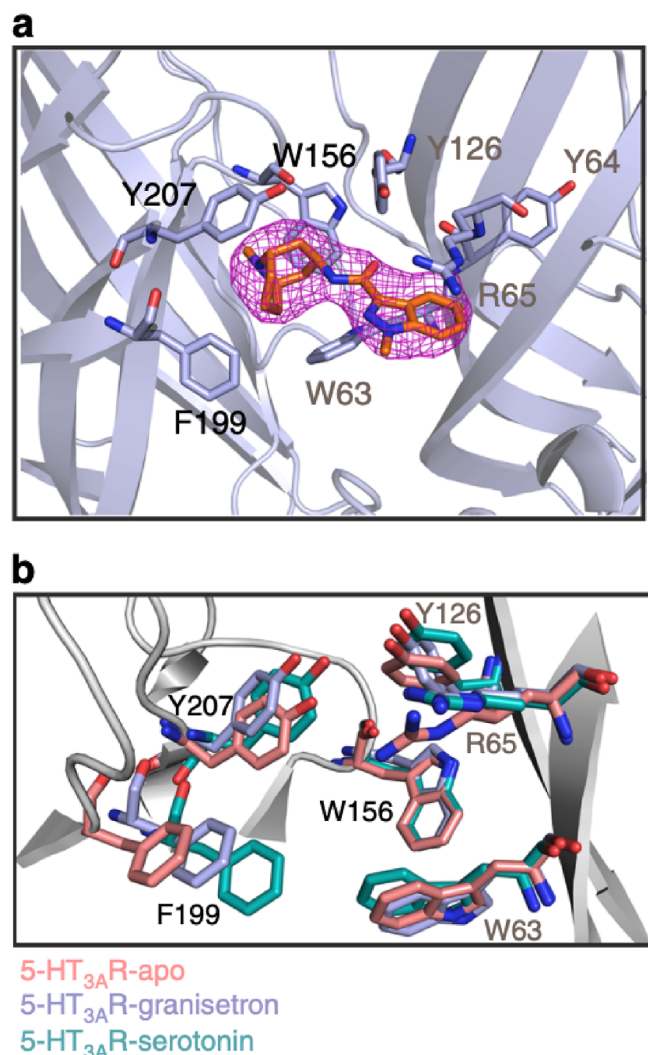
Fig. 14. The binding site of the anti-emetic drug granisetron. (a) The density map of granisetron shows the binding site located at the intersubunit interface. The residue labels on the principal subunit are marked in black and those on the complementary subunit are marked in brown. (b) A comparison of the serotonin 3A receptor-apo (5-HT3AR-apo), 5-HT3AR-granisetron, and 5-HT3AR-serotonin structures shows that residues involved in ligand-binding undergo reorientation, due to granisetron's larger size. (from[82,] their Fig 2, reprinted with permission).

between the extracellular domains of two of its subunits. Binding of these compounds may facilitate channel activation by stabilizing the interactions between the subunits. The antagonist flumazenil binds deeper into this pocket and may not be able to stabilize the interactions between the subunits.

Sodium channel. Voltage-gated sodium channel 1.5 (Nav 1.5) produces the cardiac action potential for heartbeat, and is the target of many drugs, e.g. antiarrythmic drugs such as flecainide. The cryo-EM structure of flecainide in complex with Nav 1.5 (Fig 4G)[88] reveals the detailed interactions between the compound and the channel pore, next to the selectivity filter. Other voltage-gated sodium channels are sensitive to neurotoxins such as tetrodotoxin (TTX, from the fugu fish) and saxitoxin (a paralytic shellfish toxin). The molecular basis of their pore-blocking activity has also been revealed by cryo-EM studies[89].

Potassium channel. ATP-sensitive potassium (KATP) channels in pancreatic β-cells control insulin secretion in response to blood glucose levels. They are the targets of the type 2 diabetes drug sulfonylureas, such as glibenclamide (GBC). It is bound in a central cavity of the transmembrane domain of the peripheral sulfonylurea receptor (SUR) subunit (Figs. 4H,16)[90]. The structure suggests a mechanism how binding of glibenclamide to the peripheral subunit can inhibit the central potassium channel. The carbamoylbenzoic acid drug repaglinide shares the same binding site[90–91].

Voltage-gated calcium channels. Voltage-gated calcium (Cav) channels are targets for widely used therapeutic agents. Cav1 antagonists such as dihydropyridines (DHP, with nifedipine as an example), benzothiazepines (BTZ, diltiazem), and phenylalkylamines (PAA, verapamil) are used in the clinic to treat hypertension, angina pectoris, and cardiac arrhythmia. BTZ and PAA compounds block the pore of the channel, while DHP compounds bind in an allosteric site, and some DHP compounds (Bay K 8644) are agonists. The binding modes of these compounds have been defined by cryo-EM studies (Figs. 4I,17)[92–93].

Ryanodine receptor. Ryanodine receptors (RyRs) are ligand-gated calcium channels important in muscle function; they are a therapeutic target for arrhythmia, muscular dystrophy, neurodegenerative disease, and other myopathies[94]. They are exceptionally large, and hence have been resistant to crystallography. The first cryo-EM structures were determined in 2015[95], with multiple conformational states associated with gating and binding sites of modulators (e.g. caffeine) determined one year later (Fig. 18)[96]. Ca^{2+} converts the original rigid apo state to a 'primed' (non-conducting) state, poised for activation, which then is activated for pore conduction by binding of ATP. The natural product ryanodine locks the channel in an ion-conducting state. Intriguingly, dilation of the pore occurs by bowing and distortion of the S6 helix from a point midway through the membrane. The binding site and mechanism of competitive partial agonists nucleosides and nucleotides is now clear. A small molecule, ARM210, discovered based on these structures, is in clinical trials for RyR-mediated myopathies[97].

Intasome. The HIV intasome mediates the integration of the viral genetic material into the host genome and is the target of integrase strand-transfer inhibitors (INSTIs), such as the second-generation drugs bictegravir and dolutegravir. Recent cryo-EM studies have revealed how these compounds, as well as other related molecules, are bound to integrase (Fig. 4J)[98–99], coordinating two Mg^{2+} ions in the active site. The structure of a resistant mutant in complex with bictegravir provides insights into the mechanism of resistance.

Prospects and summary: The recent revolution in cryo-EM has produced an explosion of structures at near-atomic or better resolution. Further developments in applying cryo-EM to smaller proteins, in preparing cryo-grids for data collection[100–101], and in automation of data collection and image analysis will further enhance the power and applicability of this technology. The establishment of national EM facilities should make it easier to access the top-end instruments for data collection and reconstruction at high resolution. Moreover, recent developments suggest that electron microscopes at 100 kV could be sufficient to produce high quality structures, which would reduce the cost of instruments and make them more widely available[102].

In terms of impact on drug discovery, we expect cryo-EM has the greatest future potential in cases where the advantages of cryo-EM over other structural approaches are most needed:

Where ligand binding site is unknown, and where ligand-induced conformational changes are critical for understanding mechanism, like ion channels

In cytoplasmic proteins where the target may be one or two proteins in a large oligomeric structure. This includes not only the viral proteins mentioned above, but also cases like the inflammasome[103], and the actin-myosin complex[104], microtubules[105] and the ribosome[106].

Where the SAR has seemed intractable and/or where optimization of molecules has not achieved the target profile,

where the targets are resistant to crystallization.

In focusing here on cryo-EM, we are not diminishing the impact of X-ray crystallography. The methods are complementary in many ways.
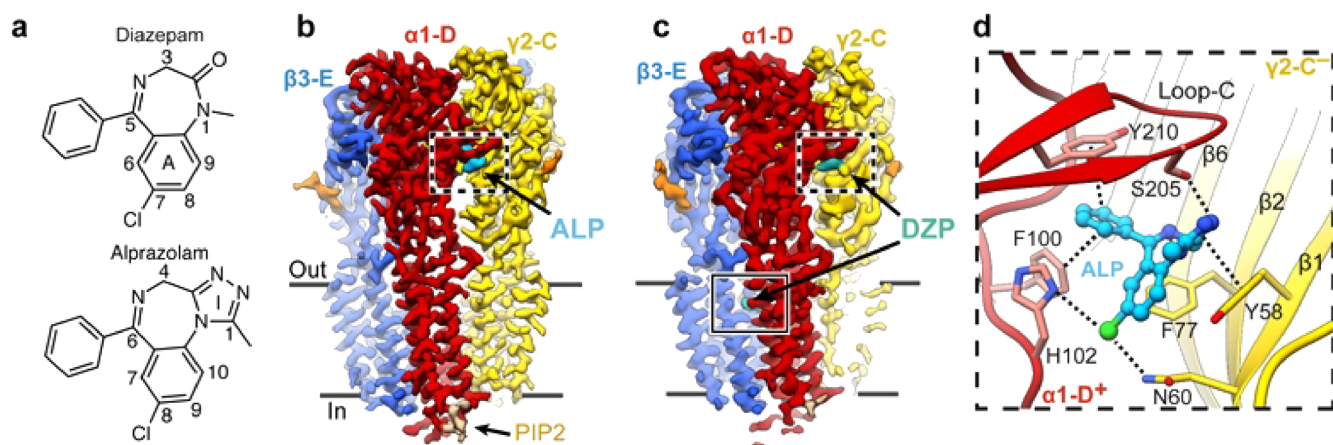
Fig. 15. The binding modes of diazepam (DZP) and alprazolam (ALP) from cryo-EM studies of Masiulis et al (from[87], their Fig 4 reprinted with permission). a. Chemical structures of DZP and ALP. b, c, Viewed parallel to the membrane plane, the cryo-EM map of the α1β3γ2 GABA$_A$ R in complex with ALP (cyan) (b) and DZP (teal) (c). d. Detailed view of the benzodiazepine binding site at the α1$^+$/γ2$^-$ interface showing ALP bound.
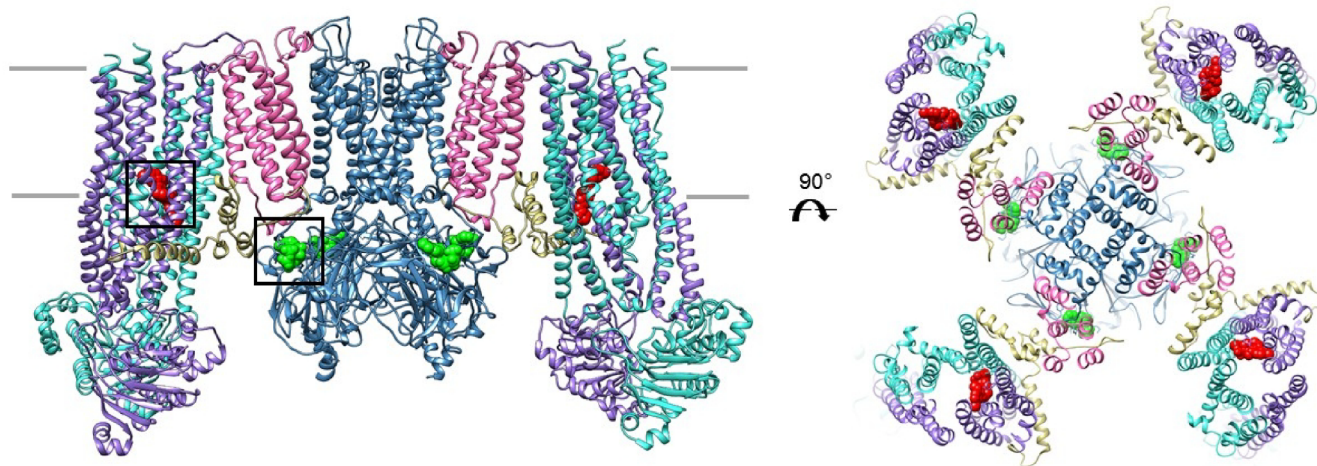

Fig. 16. The cryo-EM structure shows that glibenclamide (red) is bound in a central cavity of the transmembrane domain of the K-channel, the peripheral sulfonylurea receptor (SUR) subunit (left viewed in membrane; right from extracellular orientation). ATP is in green. (from[90], their Fig 1 reprinted with permission).

For example, the first X-ray structure of the ribosome relied on information from earlier cryo-EM structures.[4–5] Fitting cryo-EM density of large complexes often relies on X-ray structures of individual proteins, for example[70,78]. A recurring question is "in those cases where the same protein has been studied via X-ray crystallography and cryo-EM, how do those structures compare?". We are not aware of any systematic studies of this fascinating question. However, for those instances where a comparison can be made, in general the significant differences are in flexible loops on the surface, e.g.[69–70]. These loops in solution may not have a well-defined structure anyway.

Another question is whether cryo-EM will be able to support the rapid iterative cycles that crystallography is often capable of in structure-based design. At this point, there is little in the published literature that allows us to properly address that. Private communications from those performing such work in pharma R&D organizations indicates that a wave of publications is imminent, which will hopefully shed light on this issue.

The new cryo-EM structures have provided unprecedented insights into the molecular mechanisms of complex biochemical processes. They have also had a profound impact on drug discovery, defining the binding modes and mechanisms of action of well-known drugs as well

as driving the design and development of new compounds; they provide compelling opportunities for further optimization of existing molecules. Most excitingly, the latest cryo-EM technology has produced structures at 1.2 Å resolution, which demonstrates the power of this technology and should lead to resolution improvements in most cryo-EM structures. Therefore, we are convinced that cryo-EM will play an ever-increasing role in drug discovery in the coming years.

Funding

Declaration of Competing Interest

LT is a consultant for Nimbus Therapeutics and Kintor Pharmaceuticals. JVD has no conflicts, but is President of Van Drie Research, which focuses on structure-based drug discovery for small biotech firms, and whose policy is not to disclose names of clients.
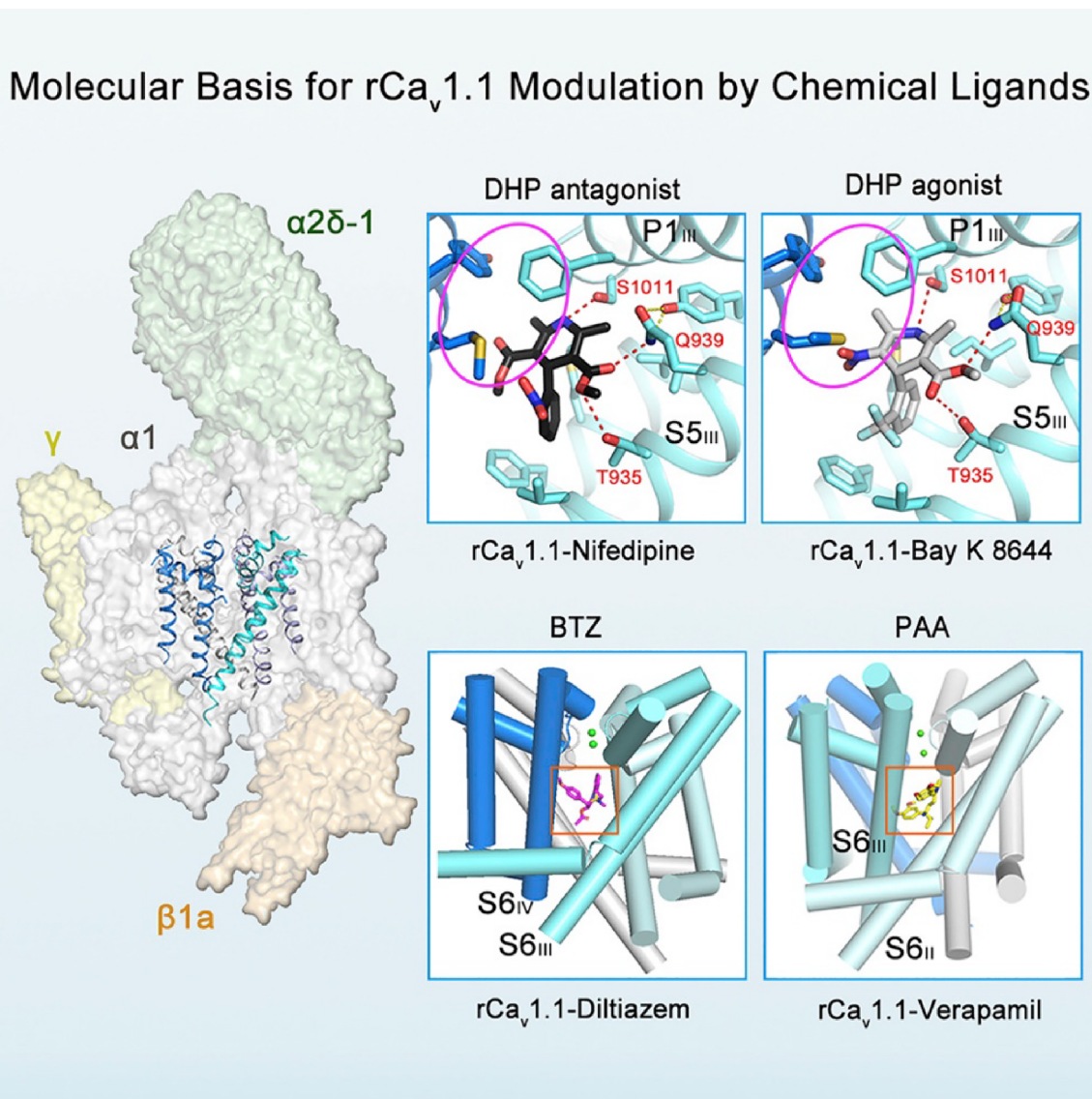
Fig. 17. Structure of CaV-1.1. A voltage-gated calcium channel CaV-1.1, with nifedipine, Bay K8644, diltiazem, and verapamil bound (from[92], reprinted with permission).
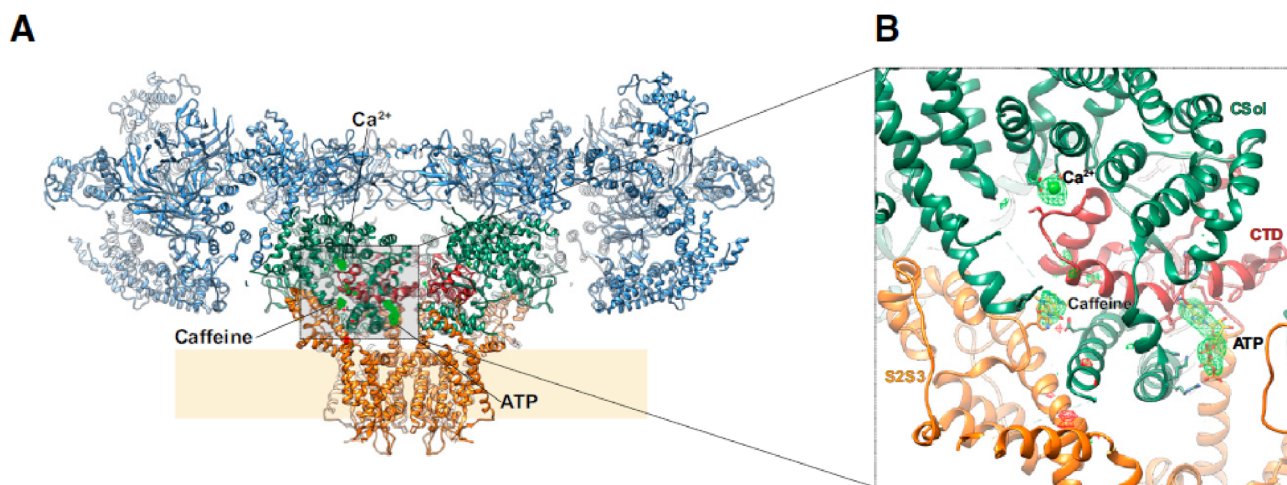
Fig. 18. Ca^{2+}, ATP, and Caffeine Bind to the C-Terminal Domain of RyR1. (A) The architecture of RyR1/Cs2 is depicted in ribbon representation, different domains color-coded. Putative binding sites for Ca2+, ATP, and caffeine are labeled. (B) Enlarged view with ligands and interacting residues on RyR1 depicted in stick representation (from Fig 2.[96], reprinted with permission).

Appendix A. Supplementary data

Supplementary data to this article can be found online at https://doi.org/10.1016/j.bmcl.2020.127524.

References

[1]. Palella FJ, et al. Declining morbidity and mortality among patients with advanced human immunodeficiency virus infection. *N Engl J Med.* 1998;338:853–860. https://doi.org/10.1056/NEJM199803263381301.

[2]. Radermacher M, Frank J. Representation of three-dimensionally reconstructed objects in electron microscopy by surfaces of equal density. *J Microsc.* 1984;136:77–85.

[3]. Frank J, Zhu J, Penczek P, et al. A model of protein synthesis based on cryo-electron microscopy of the E. coli ribosome. *Nature.* 1995;376:441–444.

[4]. Ban N, Freeborn B, Nissen P, et al. A 9 Å resolution X-ray crystallographic map of the large ribosomal subunit. *Cell.* 1998;93:1105–1115.

[5]. Ban, Nenad, Poul Nissen, Jeffrey Hansen, Peter B. Moore, and Thomas A. Steitz. "The Complete Atomic Structure of the Large Ribosomal Subunit at 2.4 Å Resolution." Science 289, no. 5481 (August 11, 2000): 905–20. https://doi.org/10.1126/science.289.5481.905.

[6]. Wilson Daniel N, Schluenzen Frank, Harms Joerg M, Starosta Agata L, Connell Sean R, Fucini Paola. The oxazolidinone antibiotics perturb the ribosomal peptidyl-transferase center and effect TRNA positioning. *Proc Natl Acad Sci.* 2008;105(36):13339.

[7]. Chandrasekaran V, Juszkiewicz S, Choi J, et al. Mechanism of ribosome stalling during translation of a poly(A) tail. *Nat Struct Mol Biol.* 2019;26(12):1132–1140. https://doi.org/10.1038/s41594-019-0331-x.

[8]. Frank J. Advances in the field of single-particle cryo-electron microscopy over the last decade. *Nat Protoc.* 2017;12(2):209–212. https://doi.org/10.1038/nprot.2017.004.

[9]. Nakane T, Kotecha A, Sente A, et al. Single-particle cryo-EM at atomic resolution. *bioRxiv.* 2020 2020.05.22.110189.

[10]. Yip KM, Fischer N, Paknia E, Chari A, Stark H. Breaking the next Cryo-EM resolution barrier – atomic resolution determination of proteins!. *bioRxiv.* 2020 2020.05.21.106740.

[11]. Fernandez-Leiro R, Scheres SHW. Unravelling biological macromolecules with cryo-electron microscopy. *Nature.* 2016;537(7620):339–346. https://doi.org/10.1038/nature19948.

[12]. Nogales E. The development of cryo-EM into a mainstream structural biology technique. *Nat Methods.* 2016;13(1):24–27. https://doi.org/10.1038/nmeth.3694.

[13]. García-Nafría Javier, Tate Christopher G. Cryo-electron microscopy: moving beyond X-ray crystal structures for drug receptors and drug development. *Ann Rev Pharmacol Toxicol.* 2020;60(1):51–71. https://doi.org/10.1146/annurev-pharmtox-010919-023545.

[14]. Subramaniam S, Earl LA, Falconieri V, Milne JLS, Egelman EH. Resolution advances in Cryo-EM enable application to drug discovery. *Curr Opin Struct Biol.* 2016;41:194–202. https://doi.org/10.1016/j.sbi.2016.07.009.

[15]. Merk Alan, Bartesaghi Alberto, Banerjee Soojay, Falconieri Veronica, Rao Prashant, Davis Mindy I, Pragani Rajan, et al. Breaking Cryo-EM resolution barriers to facilitate drug discovery. *Cell.* 2016;165(7):1698–1707. https://doi.org/10.1016/j.cell.2016.05.040.

[16]. Renaud J-P, Chari A, Ciferri C, et al. Cryo-EM in drug discovery: achievements, limitations and prospects. *Nat Rev Drug Discov.* 2018;17(7):471–492. https://doi.org/10.1038/nrd.2018.77.

[17]. Vinothkumar KR, Henderson R. Single particle electron cryomicroscopy: trends, issues and future perspective. *Q Rev Biophys.* 2016;49:e13 https://doi.org/10.1017/S0033583516000068.

[18]. Zhu J, Cheng L, Qin Fang Z, Zhou H, Honig B. Building and refining protein models within cryo-electron microscopy density maps based on homology modeling and multiscale structure refinement. *J Mol Biol.* 2010;397(3):835–851. https://doi.org/10.1016/j.jmb.2010.01.041.

[19]. Cheng Y. Membrane protein structural biology in the era of single particle cryo-EM. *Curr Opin Struct Biol.* 2018;52:58–63. https://doi.org/10.1016/j.sbi.2018.08.008.

[20]. Zivanov J, Nakane T, Forsberg BO, Kimanius D, Hagen WJH, Lindahl E, Scheres SH. New tools for automated high-resolution cryo-EM structure determination in RELION-3. *eLife.* 2018;7:e42166.

[21]. Punjani A, Rubinstein JL, Fleet DJ, Brubaker MA. cryoSPARC: algorithms for rapid unsupervised cryo-EM structure determination. *Nat Methods.* 2017;14:290–296.

[22]. Grant T, Rohou A, Grigorieff N. cisTEM, user-friendly software for single-particle image processing. *eLife.* 2018;7:e35383.

[23]. Bell JM, Chen M, Durmaz T, Fluty AC, Ludtke SJ. New software tools in EMAN2 inspired by EMDatabank map challenge. *J Struct Biol.* 2018;204:283–290.

[24]. Emsley P, Cowtan KD. Coot: model-building tools for molecular graphics. *Acta Cryst.* 2004;D60:2126–2132.

[25]. Adams PD, Grosse-Kunstleve RW, Hung L-W, et al. PHENIX: building a new software for automated crystallographic structure determination. *Acta Cryst.* 2002;D58:1948–1954.

[26]. Murshudov GN, Vagin AA, Dodson EJ. Refinement of macromolecular structures by the maximum-likelihood method. *Acta Cryst.* 1997;D53:240–255.

[27]. Wang RY, Song Y, Barad BA, Cheng Y, Fraser JS, DiMaio F. Automated structure refinement of macromolecular assemblies from cryo-EM maps using Rosetta. *eLife.* 2016;5:e17219.

[28]. Goddard TD, Huang CC, Meng EC, et al. UCSF ChimeraX: meeting modern challenges in visualization and analysis. *Protein Sci.* 2018;27:14–25.

[29]. Burke AC, Huff MW. ATP-citrate lyase: genetics, molecular biology and therapeutic target for dyslipidemia. *Curr Opin Lipidol.* 2017;28:193–200.

[30]. Granchi C. ATP citrate lyase (ACLY) inhibitors: an anti-cancer strategy at the crossroads of glucose and lipid metabolism. *Eur J Med Chem.* 2018;157:1276–1291.

[31]. Laufs U, Banach M, Mancini GBJ, et al. Efficacy and safety of bempedoic acid in patients with hypercholesterolemia and statin intolerance. *J Amer Heart Assoc.* 2019;8:e011662.

[32]. Wei J, Leit S, Kuai J, et al. An allosteric mechanism for potent inhibition of human ATP-citrate lyase. *Nature.* 2019;568:566–570.

[33]. Palczewski Krzysztof, Kumasaka Takashi, Hori Tetsuya, Behnke Craig A, Motoshima Hiroyuki, Fox Brian A, Le Trong Isolde, et al. Crystal structure of rhodopsin: A G protein-coupled receptor. *Science.* 2000;289(5480):739. https://doi.org/10.1126/science.289.5480.739.

[34]. Cherezov Vadim, Rosenbaum Daniel M, Hanson Michael A, Rasmussen Søren GF, Thian Foon Sun, Kobilka Tong Sun, Choi Hee-Jung, et al. High-resolution crystal structure of an engineered human β2-adrenergic G protein–coupled receptor. *Science.* 2007;318(5854):1258. https://doi.org/10.1126/science.1150577.

[35]. Shimada I, Ueda T, Kofuku Y, Eddy MT, Wüthrich K. GPCR drug discovery: integrating solution NMR data with crystal and cryo-EM structures. *Nat Rev Drug Discov.* 2019;18(1):59–82. https://doi.org/10.1038/nrd.2018.180 Epub 2018 Nov 9.

[36]. de Graaf C, Donnelly D, Wootten D, et al. "Glucagon-like peptide-1 and its class B G protein-coupled receptors: a long march to therapeutic successes". Edited by Richard Dequan Ye. *Pharmacol Rev.* 2016;68(4):954–1013. https://doi.org/10.1124/pr.115.011395.

[37]. Smelcerovic Andrija, Lazarevic Jelena, Tomovic Katarina, Anastasijevic Marija, Jukic Marko, Kocic Gordana, Anderluh Marko. An overview, advantages and therapeutic potential of nonpeptide positive allosteric modulators of glucagon-like peptide-1 receptor. *ChemMedChem.* 2019;14(5):514–521. https://doi.org/10.1002/cmdc.201800699.

[38]. Morris Lindsey C, Nance Kellie D, Gentry Patrick R, Days Emily L, David Weaver C, Niswender Colleen M, Thompson Analisa D, et al. Discovery of (S)-2-Cyclopentyl- N -((1-Isopropylpyrrolidin2-Yl)-9-Methyl-1-Oxo-2,9-Dihydro-1 H -Pyrrido[3,4- b]Indole-4-Carboxamide (VU0453379): a novel, CNS penetrant glucagon-like peptide 1 receptor (GLP-1R) positive allosteric modulator (PAM). *J Med Chem.* 2014;57(23):10192–10197. https://doi.org/10.1021/jm501375c.

[39]. Drucker DJ. Mechanisms of action and therapeutic application of glucagon-like peptide-1. *Cell Metab.* 2018;27(4):740–756. https://doi.org/10.1016/j.cmet.2018.03.001.

[40]. Zhang Yan, Sun Bingfa, Feng Dan, Hongli Hu, Chu Matthew, Qianhui Qu, Tarrasch Jeffrey T, et al. Cryo-EM structure of the activated GLP-1 receptor in complex with a G protein. *Nature.* 2017;546(7657):248–253. https://doi.org/10.1038/nature22394.

[41]. Deng X, Tavallaie MS, Sun R, et al. Drug discovery approaches targeting the incretin pathway. plus company reports from vTv Therapeutics, e.g. *Bioorg Chem.* 2020;99:103810 https://vtvtherapeutics.com/pipeline/ttp273/https://doi.org/10.1016/j.bioorg.2020.103810.

[42]. Zhao Peishen, Liang Yi-Lynn, Belousoff Matthew J, Deganutti Giuseppe, Fletcher Madeleine M, Willard Francis S, Bell Michael G, et al. Activation of the GLP-1 receptor by a non-peptidic agonist. *Nature.* 2020;577(7790):432–436. https://doi.org/10.1038/s41586-019-1902-z.

[43]. The Structure of the Potassium Channel: Molecular Basis of K + Conduction and Selectivity Declan A. Doyle, João Morais Cabral, Richard A. Pfuetzner, Anling Kuo, Jacqueline M. Gulbis, Steven L. Cohen, Brian T. Chait, Roderick MacKinnon Science 1998: 280 5360, pp. 69-77 DOI:10.1126/science.280.5360.69.

[44]. Gunthorpe MJ, Chizh BA. Clinical development of TRPV1 antagonists: targeting a pivotal point in the pain pathway. *Drug Discov Today.* 2009;14(1–2):56–67.

[45]. Liao M, Cao E, Julius D, Cheng Y. Structure of the TRPV1 ion channel determined by electron cryo-microscopy. *Nature.* 2013;504(7478):107–112. https://doi.org/10.1038/nature12822.

[46]. Cao E, Liao M, Cheng Y, Julius D. TRPV1 structures in distinct conformations reveal activation mechanisms. *Nature.* 2013;504(7478):113–118. https://doi.org/10.1038/nature12823.

[47]. Dawning of a new era in TRP channel structural biology by cryo-electron microscopy Madej, M. Gregor; Ziegler, Christine Pflügers Archiv European Journal of Physiology of Physiology, 470 2 2018.

[48]. Lee Y, Hong S, Cui M, Sharma PK, Lee J, Choi S. Transient receptor potential vanilloid type 1 antagonists: a patent review (2011–2014). *Expert Opin Ther Pat.* 2015;25(3):291–318. https://doi.org/10.1517/13543776.2015.1008449.

[49]. Lee, et al. Note they describe using a homology model of the human form; this was built from the rat cryo-EM structure, which has ~90% homology with the human. *Bioorg Med Chem.* 2017;25(8):2451–2462.

[50]. Ann, et al. *Bioorg Med Chem Lett.* 2016;26(15):3603–3607. https://doi.org/10.1016/j.bmcl.2016.06.010.

[51]. Identification of the cystic fibrosis gene: cloning and characterization of complementary DNA JR Riordan, JM Rommens, B Kerem, N Alon, R Rozmahel, Z Grzelczak, J Zielenski, S Lok, N Plavsic, JL Chou, et al. Science 08 Sep 1989: 245, 4922, pp. 1066-1073 DOI:10.1126/science.2475911.

[52]. Identification of the cystic fibrosis gene: genetic analysis B Kerem, JM Rommens, JA Buchanan, D Markiewicz, TK Cox, A Chakravarti, M Buchwald, LC Tsui Science 08 Sep 1989: 245, 4922, pp. 1073-1080 DOI: 10.1126/science.2570460.

[53]. Rommens JM, Iannuzzi MC, Kerem B, Drumm ML, Melmer G, Dean M, Rozmahel

R, Cole JL, Kennedy D, Hidaka N, et al. Identification of the cystic fibrosis gene: chromosome walking and jumping. *Science*. 1989;245(4922):1059–1065. https://doi.org/10.1126/science.2772657.

[54]. van Goor F, et al. Correction of the F508del-CFTR protein processing defect in vitro by the investigational drug VX-809. *PNAS*. 2011;108(46):18843–18848.

[55]. Hadida S, Van Goor F, Zhou J, et al. Discovery of N-(2,4-di-tert-butyl-5-hydroxyphenyl)-4-oxo-1,4-dihydroquinoline-3-carboxamide (VX-770, ivacaftor), a potent and orally bioavailable CFTR potentiator. *J Med Chem*. 2014;57(23):9776–9795.

[56]. Members of the discovery team were named Heroes of Chemistry by the ACS in 2013 ACS press release 9/8/13 https://www.acs.org/content/acs/en/pressroom/newsreleases/2013/september/new-heroes-of-chemistry-developed-products-that-improve-health-and-protect-food-supply.html.

[57]. Zhang Z, Chen J. Atomic structure of the cystic fibrosis transmembrane conductance regulator. *Cell*. 2016;167:1586–1597.

[58]. Liu, Zhang Z, Csanády L, Gadsby DC, Chen J. Molecular structure of the human CFTR ion channel. *Cell*. 2017;169:1–11.

[59]. Zhang Z, Liu F, Chen J. Conformational changes of CFTR upon phosphorylation and ATP binding. *Cell*. 2017;170:483–491.

[60]. Liu Fangyu, Zhang Zhe, Levit Anat, Levring Jesper, Touhara Kouki K, Shoichet Brian K, Chen Jue. Structural identification of a hotspot on CFTR for potentiation. *Science*. 2019;364(6446):1184–1188. https://doi.org/10.1126/science.aaw7611.

[61]. Dalton James, Kalid Ori, Schushan Maya, Ben-Tal Nir, Villà-Freixa Jordi. New model of cystic fibrosis transmembrane conductance regulator proposes active channel-like conformation. *J Chem Inf Modeling*. 2012;52(7):1842–1853. https://doi.org/10.1021/ci2005884.

[62]. Curran ME, Splawski I, Timothy KW, Vincent GM, Green ED, Keating MT. A molecular basis for cardiac arrhythmia: HERG mutations cause long QT syndrome. *Cell*. 1995;80:805–811.

[63]. Sanguinetti MC, Jiang C, Curran ME, Keating MT. A mechanistic link between an inherited and an acquired cardiac arrhythmia: HERG encodes the IKr potassium channel. *Cell*. 1995;81:299–307.

[64]. Farid R, Day T, Friesner RA, Pearlstein RA. New insights about HERG blockade obtained from protein modeling, potential energy mapping, and docking studies. *Bioorg Med Chem*. 2006;14(9):3160–3173. https://doi.org/10.1016/j.bmc.2005.12.032.

[65]. Wang W, MacKinnon R. Cryo-EM structure of the open human Ether-à-go-go-Related K+ channel hERG. *Cell*. 2017;169:422–430.e10.

[66]. Passini Elisa, Britton Oliver J, Hua Rong Lu, Rohrbacher Jutta, Hermans An N, Gallacher David J, Greig Robert JH, Bueno-Orovio Alfonso, Rodriguez Blanca. Human In silico drug trials demonstrate higher accuracy than animal models in predicting clinical pro-arrhythmic cardiotoxicity. *Front Physiol*. 2017;8:668. https://doi.org/10.3389/fphys.2017.00668.

[67]. Garrido A, Lepailleur A, Mignani SM, Dallemagne P, Rochais C. hERG toxicity assessment: useful guidelines for drug design. *Eur J Med Chem*. 2020;195:112290. https://doi.org/10.1016/j.ejmech.2020.112290.

[68]. Lu R, Zhao X, Li J, et al. Genomic characterisation and epidemiology of 2019 novel coronavirus: implications for virus origins and receptor binding. *Lancet (London, England)*. 2020;395(10224):565–574. https://doi.org/10.1016/S0140-6736(20)30251-8.

[69]. Walls AC, Park YJ, Tortorici MA, Wall A, McGuire AT, Veesler D. Structure, function, and antigenicity of the SARS-CoV-2 spike glycoprotein. *Cell*. 2020;181(2):281–292.e6. https://doi.org/10.1016/j.cell.2020.02.058.

[70]. Gao, Y., Yan, L., Huang, Y., Liu, F., Zhao, Y., Cao, L., Wang, T., Sun, Q., Ming, Z., Zhang, L., Ge, J., Zheng, L., Zhang, Y., Wang, H., Zhu, Y., Zhu, C., Hu, T., Hua, T., Zhang, B., Yang, X., … Rao, Z. (2020). Structure of the RNA-dependent RNA polymerase from COVID-19 virus. Science (New York, N.Y.), 368(6492), 779–782. PDB entry 6M71. DOI:10.1126/science.abb7498.

[71]. Hillen, Hauke S., Goran Kokic, Lucas Farnung, Christian Dienemann, Dimitry Tegunov, and Patrick Cramer. "Structure of Replicating SARS-CoV-2 Polymerase." Preprint. Biophysics, April 27, 2020. DOI:10.1101/2020.04.27.063180.

[72]. Hung IF, Lung KC, Tso EY, et al. Triple combination of interferon beta-1b, lopinavir-ritonavir, and ribavirin in the treatment of patients admitted to hospital with COVID-19: an open-label, randomised, phase 2 trial. *Lancet (London, England)*. 2020;395(10238):1695–1704. https://doi.org/10.1016/S0140-6736(20)31042-4.

[73]. Bartesaghi A, Merk A, Banerjee S, et al. 2.2 A resolution cryo-EM structure of beta-galactosidase in complex with a cell-permeant inhibitor. *Science*. 2015;348(6239):1147–1151.

[74]. Merk A, Bartesaghi A, Banerjee S, et al. Breaking cryo-EM resolution barriers to facilitate drug discovery. *Cell*. 2016;165(7):1698–1707.

[75]. Bartesaghi A, Aguerrebere C, Falconieri V, et al. Atomic resolution Cryo-EM structure of beta-galactosidase. *Structure*. 2018;26(6):848–856.e3.

[76]. Borgnia MJ, Banerjee S, Merk A, et al. Using Cryo-EM to map small ligands on dynamic metabolic enzymes: studies with glutamate dehydrogenase. *Mol*

[77]. *Pharmacol*. 2016;89(6):645–651.

[77]. Saur M, Hartshorn MJ, Dong J, et al. Fragment-based drug discovery using cryo-EM. *Drug Discov Today*. 2019.

[78]. Wong W, Bai XC, Brown A, et al. Cryo-EM structure of the Plasmodium falciparum 80S ribosome bound to the anti-protozoan drug emetine. *eLife*. 2014;3:e03080.

[79]. Juza R, Vlcek P, Mezeiova E, Musilek K, Soukup O, Korabecny J. Recent advances with 5-HT3 modulators for neuropsychiatric and gastrointestinal disorders. *Med Res Rev*. 2020.

[80]. Basak S, Gicheru Y, Rao S, Sansom MSP, Chakrapani S. Cryo-EM reveals two distinct serotonin-bound conformations of full-length 5-HT3A receptor. *Nature*. 2018;563:270–274.

[81]. Polovinkin L, Hassaine G, Perot J, et al. Conformational transitions of the serotonin 5-HT3 receptor. *Nature*. 2018;563:275–279.

[82]. Basak S, Gicheru Y, Kapoor A, Mayer ML, Filizola M, Chakrapani S. Molecular mechanism of setron-mediated inhibition of full-length 5-HT3A receptor. *Nat Commun*. 2019;10:3225.

[83]. Nakagawa T. Structures of the AMPA receptor in complex with its auxilliary subunit cornichon. *Science*. 2019;366:1259–1263.

[84]. Kunugi A, Tanaka M, Suzuki A, et al. TAK-137, an AMPA-R potentiator with little agonistic effect, has a wide therapeutic window. *Neuropsychopharmacology*. 2018.

[85]. Smart TG, Stephenson FA. A half century of gamma-aminobutyric acid. *Brain Neurosci Adv*. 2019;3 2398212819858249.

[86]. Zhu S, Noviello CM, Teng J, Walsh RM, Kim JJ, Hibbs RE. Structure of a human synaptic GABAA receptor. *Nature*. 2018;559:67–72.

[87]. Masiulis S, Desai R, Uchanski T, et al. GABA$_A$ receptor signalling mechanisms revealed by structural pharmacology. *Nature*. 2019;565:454–459.

[88]. Jiang D, Shi H, Tonggu L, et al. Structure of the cardiac sodium channel. *Cell*. 2020;180(1):122–134.e10.

[89]. Shen H, Liu D, Wu K, Lei J, Yan N. Structures of human Nav1.7 channel in complex with auxilliary subunits and animal toxins. *Science*. 2019;363:1303–1308.

[90]. Martin GM, Kandasamy B, DiMaio F, Yoshioka C, Shyng SL. Anti-diabetic drug binding site in a mammalian KATP channel revealed by cryo-EM. *eLife*. 2017;6:e31054.

[91]. Ding D, Wang M, Wu JX, Kang Y, Chen L. The structural basis for the binding of repaglinide to the pancreatic KATP channel. *Cell Rep*. 2019;27:1848–1857.

[92]. Zhao Y, Huang G, Wu J, et al. Molecular basis for ligand modulation of a mammalian voltage-gated Ca2+ channel. *Cell*. 2019;177:1495–1506.

[93]. Zhao Y, Huang G, Wu Q, et al. Cryo-EM structure of apo and antagonist-bound human Cav3.1. *Nature*. 2019;576:492–497.

[94]. Zalk R, Clarke OB, des Georges A, Grassucci RA, Reiken S, Mancia F, Hendrickson WA, Frank J, Marks AR. Structure of a mammalian ryanodine receptor. *Nature*. 2015;517(7532):44–49. https://doi.org/10.1038/nature13950.

[95]. Santulli G, Lewis D, des Georges A, Marks AR, Frank J. Ryanodine receptor structure and function in health and disease. *Sub-Cell Biochem*. 2018;87:329–352. https://doi.org/10.1007/978-981-10-7757-9_11.

[96]. Amédée des Georges, Oliver B. Clarke, Ran Zalk, Qi Yuan, Kendall J. Condon, Robert A. Grassucci, Wayne A. Hendrickson, Andrew R. Marks, Joachim Frank, Structural Basis for Gating and Activation of RyR1, Cell, 167, 2016, 145-157.e17, DOI:10.1016/j.cell.2016.08.075.

[97]. https://clinicaltrials.gov/ct2/show/NCT04141670.

[98]. Cook NJ, Li W, Berta D, et al. Structural basis of second-generation HIV integrase inhibitor action and viral resistance. *Science*. 2020;367(6479):806–810.

[99]. Passos DO, Li M, Jozwik IK, et al. Structural basis for strand-transfer inhibitor binding to HIV intasomes. *Science*. 2020;367(6479):810–814.

[100]. Carragher B, Cheng Y, Frost A, et al. Current outcomes when optimizing 'standard' sample preparation for single-particle cryo-EM. *J Microsc*. 2019;276:39–45.

[101]. Han H, Fan X, Wang H, et al. High-yield monolayer graphene grids for near-atomic resolution cryoelectron microscopy. *Proc Natl Acad Sci U S A*. 2020;117:1009–1014.

[102]. Naydenova K, McMullan G, Peet MJ, et al. CryoEM at 100 keV: a demonstration and prospects. *IUCrJ*. 2019;6:1086–1098.

[103]. Jeffrey D. Nanson, Md. Habibur Rahaman, Thomas Ve, Bostjan Kobe, Regulation of signaling by cooperative assembly formation in mammalian innate immunity signalosomes by molecular mimics, Seminars in Cell & Developmental Biology, 99, 2020, Pages 96-114, ISSN 1084-9521, DOI:10.1016/j.semcdb.2018.05.002.

[104]. von der Ecken J, Müller M, Lehman W, Manstein DJ, Penczek PA, Raunser S. Structure of the F-actin-tropomyosin complex. *Nature*. 2015;519(7541):114–117. https://doi.org/10.1038/nature14033.

[105]. Wang HW, Nogales E. Nucleotide-dependent bending flexibility of tubulin regulates microtubule assembly. *Nature*. 2005;435(7044):911–915. https://doi.org/10.1038/nature03606.

[106]. Svidritskiy, Egor, Garbriel Demo, and Andrei Korostelev. "Mechanism of Premature Translation Termination on a Sense Codon." Journal of Biological Chemistry, 2018. DOI:10.1074/jbc.AW118.003232.